Quantifying Cellular Mechanotransduction in Morphogenesis and Cancer

---

A Thesis
Presented to
The Division of Mathematics and Natural Sciences
Reed College

In Partial Fulfillment
of the Requirements for the Degree
Bachelor of Arts

Abrar Ali Abidi

May 2016

Approved for the Division
(Physics)

Daniel Borrero

Acknowledgements

I could not have wished for a better team of advisors than Derek Applewhite from Biology and Daniel Borrero from Physics. Derek has from the start been a supremely generous, patient, and kind mentor. The fact that he approved of this project and gave me a place in his lab is testament enough to these qualities; the fact that he has become such a wonderful friend shows how much further they extend. Daniel gave me, whenever needed, his constant help and encouragement, in a project that lay far outside his own area of expertise. I count my lucky stars that he never tried to wave the departmental flag, and saw in this project the same sense of adventure as I did. This thesis was made at least eighteen times more readable by his discerning eye and relentless red ink.

At the beginning of this project, Greta Glover was nothing short of an angel, volunteering her time to teach me everything I needed to know about using my hands carefully, safely, and responsibly. It is from her that I learned everything I now know about experimenting and lab technique. As with Greta, none of this would have been possible without Jay Ewing, who swooped in with his magical hands whenever I needed something to be built. I thank the two of them from the bottom of my heart.

In my case, Reed saved the best for last. The friends I made this year are the ones I will cherish most once I leave. Emily Merfeld, Lily Ben-Avi, Vikram Chan-Herur, Meghan OConnell, Mari Cobb, Wick Perry, and many more. I will miss you beyond words, and I sincerely hope you all stay in my life.

I thank Rachel, whose sustained stream of love and support could always lift me from any depth. And finally I thank my family, on whose love, throughout this long and winding journey, I could always rely.

This study was supported in part by the Reed College Undergraduate Research Initiative Grant.

Table of Contents

List of Tables

List of Figures

Abstract

Traction force microscopy (TFM) is a technique that provides detailed dynamical profiles of the mechanical behavior of cells as they crawl over a gel substrate. This method, drawing on techniques and knowledge from physics and cell biology, offers to provide a force-centric view of cells that can be used to address questions in such diverse fields as developmental and cancer cell biology. I successfully established TFM as an assay at Reed, providing a tool to probe cellular mechanotransduction in contractile cells. The results of my experiment testify to the high precision and quantitative rigor that this method brings to bear on biological processes that, until recently, had only been studied qualitatively and descriptively.

Dedication

I dedicate this thesis to Falco, who is not only the most handsome German Shepherd to walk this planet, but also my bosom friend, my loyal companion, my silent partner, and my brother. Through all these years at Reed, through the best of times, through the worst of times, and through everything in between, the thought of your presence, august and stately, benign and wise, watchful and warm, has shone light on even the coldest and grayest of days like a constant, gentle sunshine.

Introduction

All animals arise and develop from an individual, intrepid, often indiscernibly small fertilized egg. Throughout this year, this fact has left me with a feeling of unmitigated awe. Every cell that makes up our body contains the same DNA, the same genetic blueprint. And yet, if I were to pluck a cell from my cheek and a cell from my brain, they would appear, if compared under a microscope, as different as a pigeon from a peacock. How is it that the same DNA molecule gives rise to so many different shapes, so many different forms and functions? In the human body alone, there are at least 200 different types of cells, and roughly 37 trillion cells in total. This enormous menagerie originates at conception with a single lonely, determined cell, which undertakes a series of divisions that gradually splinter out and form all the different cell types that we see. Meanwhile, as they differentiate and grow in number, these cells somehow meticulously and consistently arrange themselves over time, compartmentalizing first into tissues, then organs, and eventually a completed animal body [1]. There has been heroic progress over the last half-century to observe and comprehend the details of this process. And yet, the field of developmental biology still contains so many of the great unanswered scientific questions of our time [2]. Much remains to be discovered.

My investigations and the experiments described in this thesis set out to tell two stories, both from an unusual perspective. In one story, we look at the frail, diaphanous wings of the common fruit fly, a marvel of so many billions of years of evolution. In the other story we look at something darker, shadowed by death, in which the same process that helps to shape the fly's wing goes terribly awry, and one renegade cell causes a cancer to metastasize. As someone trained in physics who has recently stumbled (neither wisely nor well) into the very different world of biology, I hope to address from a different point of view these two stories, which initially meander like two winding paths, but eventually converge on the idea of forces. In the two cases I study, the forces in question lead sometimes to an animal's death, but also, sometimes, help shape the unfathomably complicated processes that lead to complex life.

0.1 Multicellular Development is Complicated but Comprehensible

Nightingales and narwhals, jellyfish and junipers—all these multicellular lifeforms begin as a single cell. Once that first cell, the egg, is fertilized, the process of develop-

ment takes over. This process, highly complex yet highly regulated, differs somewhat among the various kingdoms of life, but shares a number of fundamental characteristics. All multicellular development, for one, involves a progression of steps taken by that first cell, where it divides repeatedly, forming a large and varied palette of cells that, during this ongoing cycle of division, arranges itself into a pattern at once organized and precise. The field of developmental biology attempts to understand this process in molecular and cellular terms [3].

For the most part, multicellular development comes down to four fundamental processes as shown in Figure 1: cell proliferation, cell differentiation (or specialization), cell-cell interactions, and cell migration (or movement) [1]. As the early embryo develops, these four processes take place in a complex, interconnected web of interactions. The truly remarkable thing about this phenomenon is the total absence of any central commanding authority, which guides the behavior and fate of each cell. The cells themselves probe their surroundings and effectively decide on how they will contribute to forming the animal's body plan, carving specialized niches for themselves by selectively turning on and off different parts of their chromosomes [4]. At each of the innumerable junctures in this network of interactions, a cell chooses how to proceed from a limited set of options. These choices are largely governed by the given interior state of a cell and its interactions with adjacent cells. Like moving chess pieces, these choices progress sequentially—the branches of the network extend, intersect, and fold, with each future choice dependent on the history of choices embodied in that branch [5].

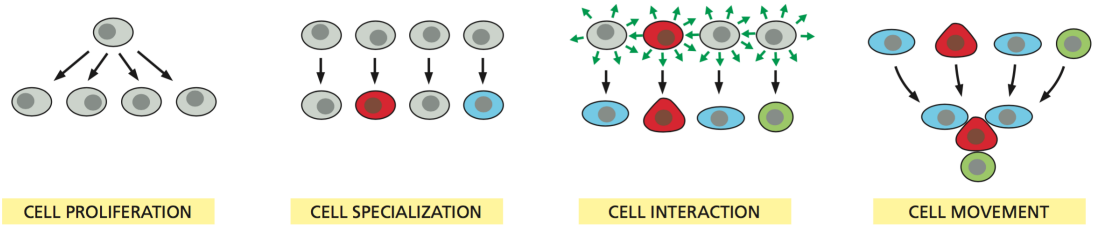

Figure 1: **The four fundamental processes that guide multicellular development.** Image reprinted from [1].

As cells differentiate, changing from one cell type to another, they take on altered shapes, and interact differently with their environments and with nearby cells. In a process called morphogenesis, these cells then rearrange themselves by migrating to different positions on the embryonic body, patterning themselves into what become distinct tissues and organs. In recent decades, morphogenesis has come to be understood as a highly mechanical process, guided in large part by forces exerted by individual cells as they crawl along stiffer or softer substrates [6]. I will return to this theme later.

0.2 Cancer is Multicellular Development Gone Awry

Our tissues have evolved exquisite mechanisms by which they renew and repair themselves. These mechanisms allow our body to withstand a remarkable degree of wear and tear. This ability of self-renewal, however, comes at a cost. When the machinery that guides this process goes awry, the result is often the genesis of a cancer. Among the great, menacing problems of our time, cancer currently causes the death of one in five people in North America [7].

Cancer is not a single disease, but a word used to describe when three different processes occur in sequence: cell proliferation, cell invasion, and metastasis. For example, if only the first of these processes—unchecked, rapid cell proliferation—takes place in some part of a human body, that alone might only result in a benign tumor, which can usually be easily removed. The real trouble begins when that tumor acquires the ability to invade other tissues. The tumor is then said to change from a benign to a malignant state. Malignant tumors, it follows, often metastasize, invading other regions of the body where they settle, form new habitations, and once again begin dividing uncontrollably. As these malignant tumors spread across the body, they can become extremely difficult—and in many cases impossible—to treat [1].

Cancer is, at its heart, a genetic disease. Cancer occurs when the mechanisms of DNA replication and repair, which allow an organism to develop and, once developed, maintain life, go amiss [8]. As a cell's DNA is replicated before division, mutations inevitably occur, where an incorrect nucleotide (an individual unit on the genome) takes the place of the correct one. These mutations, if inherited by the progeny cells, can cause faulty behavior or even cell death, though often they are harmless. Fortunately, the DNA repair machinery ensures that mistakes like these rarely occur—so infrequently, in fact, that on average a mistake eludes the DNA repair machinery for one in every 10^9 or 10^{10} nucleotides that are copied. However, given that with age the cell's machinery for replication and repair degrades, and given the trillions of cells that exist in a human body, mutations eventually accumulate [1].

When a threshold number of these mutations build up, the cell becomes cancerous, as shown in Figure 2. These mutations cannot be random, but must occur on special genes (certain stretches of DNA) on the genome [9]. These special, cancer-causing genes typically come in two varieties: proto-oncogenes and tumor suppressor genes. When proto-oncogenes undergo a mutation that causes them to be hyperactive, they turn into oncogenes, which contribute to cancer. On the other hand, when tumor suppressor genes are mutated such that their normal activity is disrupted, they too help bring about cancer. Once enough—some argue at least 10—proto-oncogenes and tumor suppressor genes are mutated in these ways, the cell emerges cancerous, and the hallmarks of that disease become manifest [10].

Cell proliferation, the first trait of a cancer, has been exhaustively studied and is relatively well understood [11]. Far less understood are cancer's two other traits–cell invasion and metastasis, both illustrated in Figure 3. Though these two phenomena are sometimes lumped together in the word "metastasis," it is necessary here to define them more precisely. Cell invasion refers to the cells that, once an initial tumor has formed, break free from their source, migrate away, and encroach on other tissues.

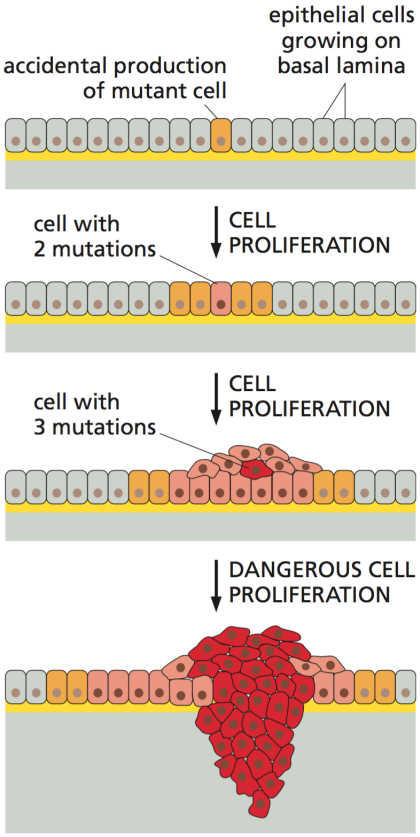

Figure 2: **The genesis and evolution of a cancer.** Here we see that accumulations of mutations, which in turn trigger rapid proliferation, give rise to malignancy. In the final frame, we see the beginning of a tumor, which has broken through the underlying protein membrane and threatens to metastasize. Image reprinted from [1].

The secondary tumors that form when such a cell has successfully invaded some other region of the body are referred to as metastases. It is worth noting that the vast majority of invasive cells do not reach their destinations. Recent studies have shown that fewer than one in thousands, perhaps fewer than one in millions, of invasive cells make it to their target site and successfully form metastases. But all it takes is one of these cells to complete its journey before all is amok in the body, and the chances of the organism's dying increase dramatically [12].

To illustrate just how little we know about cell invasion and metastasis, I quote Robert Weinberg, perhaps the preeminent cancer researcher in the world: "Our understanding of metastasis is still fragmentary. The principles that guide the migratory routes of most cancer cells are, for the moment, as mysterious as those that guide the monarch butterfly. For the cancer researcher, the process of metastasis remains a terra incognita, still largely unexplored" [13]. It goes without saying now, that any paradigmatic changes in our treating of cancer will likely follow only when we form a far more comprehensive and precise understanding of cell invasion and metastasis [12].

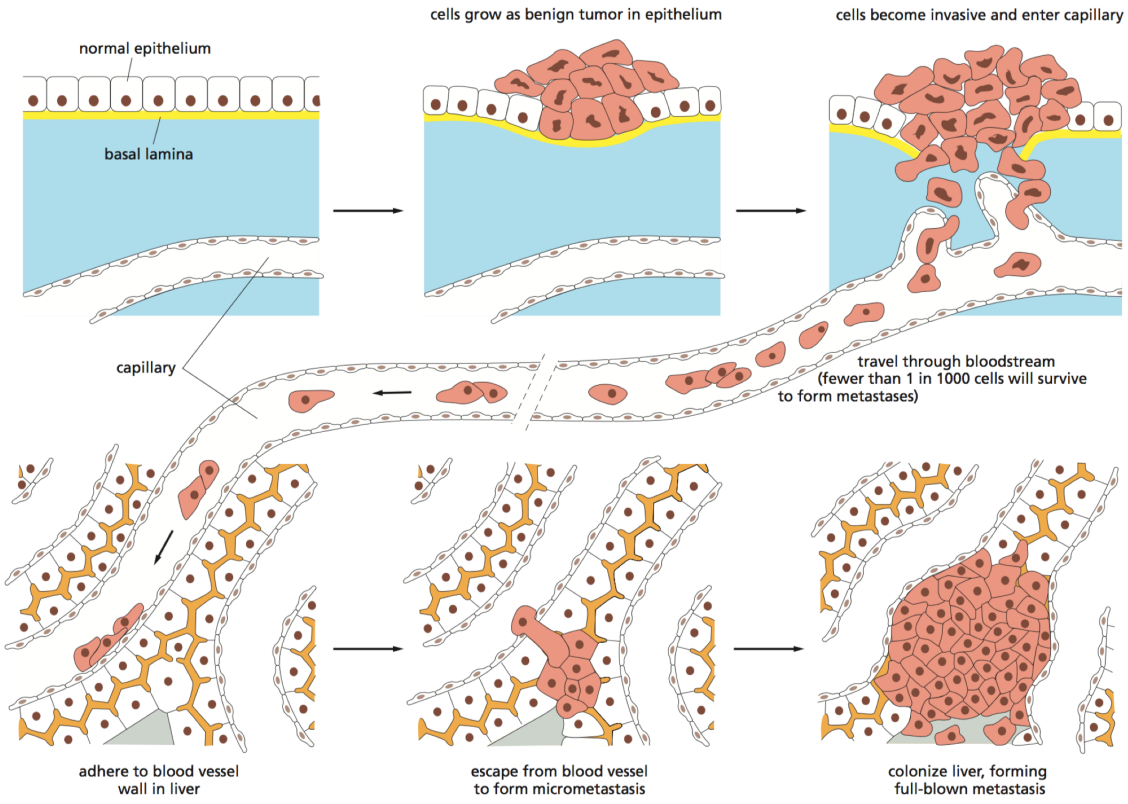

Figure 3: **Cell invasion and metastasis, in this case from the bladder to the liver.** Invasive cancer cells, once broken off from the primary tumor, enter the bloodstream and travel toward their target site. Once their, they adhere to the blood vessel wall and infiltrate the tissue, forming a metastatic, secondary tumor. Image reprinted from [1].

0.3 Mechanotransduction Connects the Outside of a Cell to its Inside

Both of the processes described in the previous two sections require that cells be able to migrate. To enable this, cells secrete a fibrous, filamentous mixture of proteins called the extracellular matrix (ECM). A cell grips the ECM by way of large protein complexes that cross its membrane called focal adhesions. Focal adhesions connect the outside of a cell to its inner machinery. Without focal adhesions, a cell could never crawl upon a substrate [1]. Much more than acting as simple gripping mechanisms, focal adhesions also act as environmental sensory organs in a process known as mechanotransduction. This process describes how cells respond differently to different stiffnesses of the ECM underlying their adhesions. When cells attach to more rigid ECM, the substrate underneath resists their pulling forces. Focal adhesions, in turn, respond to this increased tension by triggering a chemical signalling cascade, which results in the recruitment of additional proteins to deploy more focal adhesions

at the sites of increased tension. With more focal adhesions, the cell can far more effectively crawl over a stiffer substrate [14].

But the process of mechanotransduction, as has only recently begun to be understood, is far more interesting than implied by the description above. The regulation of the genome—that is, the way in which a cell turns on and off different parts of its genome—has traditionally been understood in terms of responses to simple chemical cues. What has been left largely unstudied is the way in which mechanical cues from outside the cell trigger a huge diversity of biochemical responses within it, stimulating a response in the cell far more complicated than simply the deployment of additional focal adhesions [14]. Recent studies have even offered clues that one of the major drivers behind the processes described previously, morphogenesis and cancer cell invasion, could be mechanotransduction itself [6, 15]. It follows that if mechanotransduction is mainly guided by stiffnesses of the underlying substrate, then it is highly likely that substrate stiffness plays a crucial role in determining the course of development and malignancy. We also know that both in cell differentiation and in cancer cell invasion, proteins that are critical in regulating adhesions, ECM, and the cytoskeleton are drastically altered [16, 17]. From the perspective of mechanical forces, these processes can be seen as disorders of mechanotransduction, possibly giving us a new paradigm by which to study and interpret them. With the advent of techniques to precisely measure these forces, the time is ripe for biologists to turn their energies toward understanding the causes and implications of mechanotransduction.

0.4 The Goals of this Thesis

While the correlation between substrate elasticity and mechanical forces generated by the cell has been surveyed across a range of cellular types and environments, these studies have remained largely descriptive [18]. In order for the first steps to be taken toward whole-cell quantitative models, to gain a predictive rather than merely descriptive understanding of cellular behavior, the field of cell biology calls for more precise and quantitative measurements of cellular phenomena [19]. This is where experimental physicists have brought their experience to bear on the subject. Thanks to the efforts of these physicists, atomic force microscopes and optical tweezers have become routine in studies where cells are subjected to minute, controlled forces [20, 21], but far less attention has been paid to the arguably more pressing questions concerning forces that cells themselves exert on their surroundings. An ingenious and quite recent technique devised by physicists known as traction force microscopy has emerged as a response to this problem [22, 23].

Traction force microscopy (or TFM), illustrated in Figure 4, involves embedding fluorescent beads within elastic gel matrices and measuring the movements of these beads as individual cells crawl upon the surface of the gel. By measuring the displacements of these beads, and with some knowledge of the mechanical properties of the gel, such as its thickness and stiffness, we can determine the forces that deformed the gel in the first place and caused the fluorescent beads to move. Furthermore, by chemically altering the stiffness of the gels, one can simulate different cellular en-

vironments and gain a quantitative understanding of how the cell's behavior at the cell-matrix level changes in these different contexts. Nevertheless, TFM is relatively difficult to implement, and has so far largely been practiced only in a small number of labs. In fact, with few exceptions (e.g. [24]), TFM has almost entirely eluded attempts to quantitatively measure the forces inherent in a cell's migrating journey during morphogenesis, or the forces that characterize a cancer cell's transition from non-invasive to invasive.

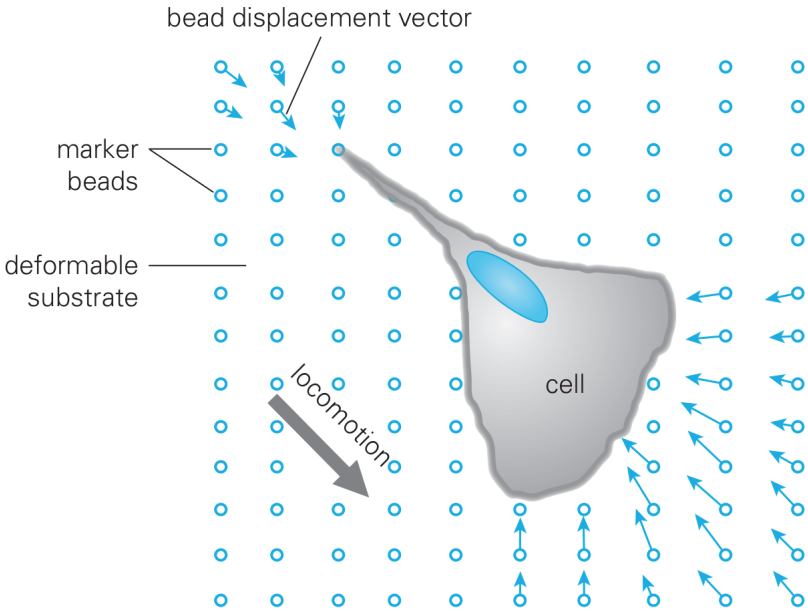

Figure 4: **Traction force microscopy.** As a cell crawls overhead, the gel deforms, dragging along the fluorescent beads within it. The movements of these beads can be tracked as displacement vectors, displaying the dynamic behavior of the cell. These vectors can then be resolved into the lateral traction forces that the cell exerts at the cell-matrix boundary. Image reprinted from [25].

My primary goal was to introduce and streamline TFM as an assay to probe cellular mechanotransduction at Reed. This involves not only getting this notoriously knotty experiment to work, but also writing and optimizing code to allow future students to quickly input their images of bead displacements, and automatically get out the traction force fields characterizing the cell's movement. I will argue for the central role that TFM must play in introducing a quantitative, mechanically-oriented paradigm to biology, to complement the gene-centric view that has dominated the subject for the last half-century. From this perspective, morphogenetic migration and increased metastatic potential can be seen to emerge from the different forces a cell exerts on substrates of varying stiffnesses. Thus, I hope not only to introduce a powerful new technique to Reed that can establish possible future collaborations between the Biology and Physics departments, but also to demonstrate that, from the point of view of forces, morphogenesis and metastasis, two subjects rarely studied

in the same context, become closely related manifestations of the same phenomenon, which in one case helps create life, and in the other, destroys it.

The rest of this thesis is organized as follows. Chapter 1 provides details of all the relevant biological knowledge for the reader to understand cellular processes such as mechanotransduction, morphogenesis, and metastasis. Chapter 2 presents the statistical techniques and physical theory used both to track particles and to calculate traction stresses in TFM. Chapter 3 provides a detailed outline and protocol of the materials and experimental design of my TFM setup. Finally, Chapter 4 is dedicated to displaying some of my results, as well as enumerating and discussing the saga of failures that led, at last, to the success of my experiment.

Chapter 1

The Biological Minimum

This section is designed to bring the reader with very little or no knowledge of biology up to speed with the relevant biological ideas and problems investigated in my thesis. As such, I begin at the very beginning, describing cells, proteins, and genes, before diving into the more complicated topics that motivated my thesis. I have tried to eschew jargon wherever it may appear, and I have striven to define all the necessary biological terms. The citations provide an extremely handy list of references for the reader who desires detail beyond what I have been able to provide here.

1.1 All Cells Share a Common Construction

While cells can differ enormously in form and function, they all share a number of common features. For one, with very few exceptions, they are tiny—typically a few dozen microns in diameter. Cells possess a nucleus, usually roundish in shape, that carries its genetic material in the form of DNA. Everything other than the nucleus is called the cytoplasm, which is surrounded by a thin membrane that contains and protects the cell. Cells take in food and convert it into usable energy. By metabolizing this energy, they coordinate all sorts of intra-cellular activities. These can be anything from enabling simple chemical reactions, to utilizing small molecular motors to move cargo across the cell, to causing the entire cell to dramatically change shape, migrate, and chase a chemical cue. Cells also use this energy to replicate themselves, copying their genetic material and dividing in two [26]. A basic outline of the structure of a cell is shown in Figure 1.1.

1.1.1 The cytoskeleton allows cells to change shape

Within the cell's cytoplasm is an intricate network of protein filaments that, among other functions, allows the cell to deform, migrate, and organize its interior. This network of proteins, called the cytoskeleton, is dynamic and constantly responding to the cell's internal and external environment. The cytoskeleton consists of three different types of mechanically distinct filaments, all shown in Figure 1.2: intermediate filaments, made up of a family of fibrous proteins; microtubles, made up of the protein

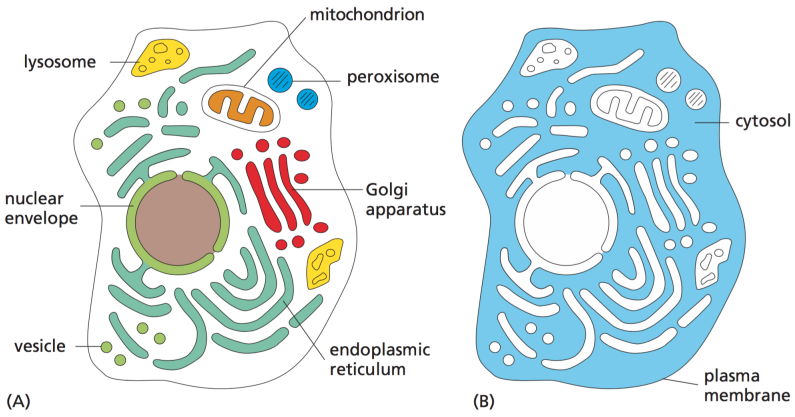

Figure 1.1: **A simplified cartoon of a cell.** (A) Membrane-enclosed organelles within the cytoplasm. (B) The cytosol, a rich mixture of chemicals dissolved in water, which permeates the cytoplasm. Image reprinted from [1].

tubulin; and actin filaments, made up of the protein actin. Intermediate filaments, durable and robust, mainly provide cells with mechanical strength when they are subjected to forces and stresses. Microtubules, which are hollow and fairly stiff, allow the cell to organize itself by providing a network of tracks along which cellular cargo can be transported. Lastly, actin filaments, which are thin and flexible, give cells the ability to move [1].

1.1.2 Three fundamental tasks govern cell motility

When we observe a migrating cell up close, we see that it extends protrusions from its membrane that appear to reach out and grab a bit of the surface in front of it. These particular protrusions are called the leading edge, that is, the edge that grows in the direction of the cell's motion. As this happens, we can see that a bit of the cell from behind, the trailing edge, appears to lift up and let go of the surface underneath, so as to roll forward and rejoin into the bulk of the cell. As the cell successively grabs the substrate before it and releases the surface behind it, the area that the cell covers on the substrate comes, on average, quite near to remaining fixed. The cell only begins to crawl by temporarily breaking and resuming this two-dimensional symmetry between itself and the surface over which it migrates [27].

The phenomenon of cell crawling, thus, is governed by three primary mechanisms, shown in Figure 1.3: protrusion, attachment, and traction. Protrusion occurs when the cell extends projections from the leading edge of the plasma membrane. Attachment describes how the cell grips onto the substrate beneath it, and how the protrusions can grab onto the substrate beyond. Traction describes how, when the cell releases its grip from the trailing edge, the cell's bulk is drawn forward [1]. The remainder of this section will outline the molecules that allow the cell to accomplish these three fundamental tasks.

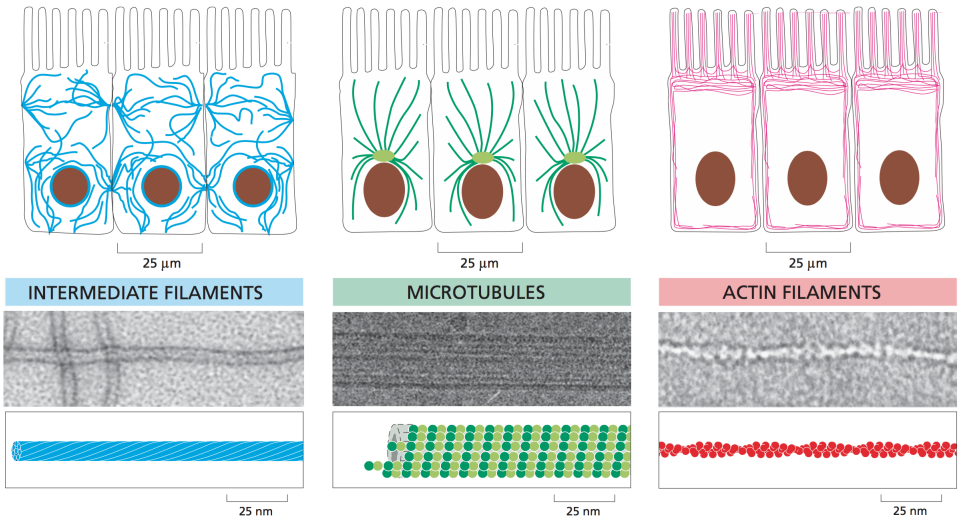

Figure 1.2: **Three columns, each illustrating one of the three proteins that make up the cytoskeleton.** At the top of each column is a diagram of the spatial distribution of that particular cytoskeletal component within the cell. Below is an electron micrograph of that component, and below that, an idealized representation of the polymer. Intermediate filaments, shown in blue, are very flexible, ropelike fibers made of intermediate filament proteins, which span the cell and give it mechanical strength to resist stress and deformations. Microtubules, shown in green, are hollow cylinders composed of the protein tubulin, which typically extend out from complexes known as centrosomes and help organize the interior of cells. Actin filaments, shown in red, wind in a helical fashion and are composed of the protein actin, forming into bundles and two- and three-dimensional networks that largely localize beneath the membrane of the cell. Image reprinted from [1].

1.2 Three Proteins are our Key Players

Proteins are the building blocks of all cells. Proteins called enzymes speed up the rates at which crucial reactions in the cell take place. Proteins that line the outer cell membrane allow important molecules to be transported to and from the cell's interior. Some proteins carry molecular signals from one cell to another, and others allow the cell to sense and respond to its environment. There is an enormous range of functions—far too many to list here—that proteins carry out within a cell.

The central dogma of molecular biology, illustrated in Figure 1.4 is simple: DNA goes to RNA goes to protein. DNA is made up from four types of nucleotides—adenine, cytosine, thymine, guanine (A, C, T, G)—that assemble in long polymer chains, and then bind via weak non-covalent interactions to another strand with complementary nucleotides. These two strands then twist around each other like a spiral staircase. DNA begets RNA in a process called transcription. RNA is also made up from four different nucleotides (A, C, U, G), three of which are the same as those in DNA, except with a slightly different chemical backbone, and one of which, uracil, is unique to RNA. Unlike DNA, RNA remains single-stranded. Finally, RNA begets

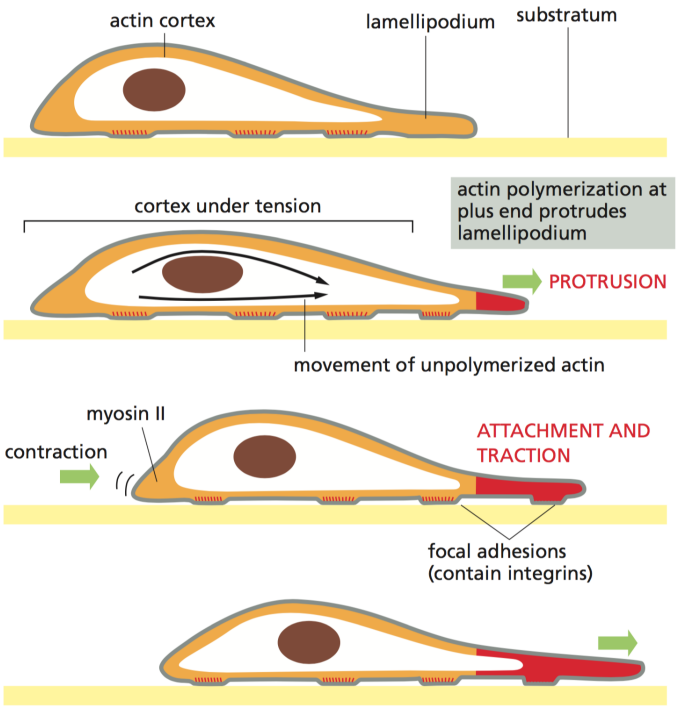

Figure 1.3: **The process of cell migration.** A sheet-like actin projection called the lamellipodium allows the cell to protrude forward. By successively attaching at the leading edge, and detaching at and retracting from the trailing edge, the cell crawls forward. Image reprinted from [1].

proteins in a process called translation. Proteins are made up of amino acids, of which 20 different types exist, strung one to another in long polymer chains. The order of the amino acids is central to the way that a protein folds up on itself via non-covalent interactions to create a large, functioning structure that can carry out a specific task [28]. The rest of this section is dedicated to understanding three particular proteins I have chosen for their importance in cell contractility and mechanotransduction.

1.2.1 Actin filaments form dynamic networks

We have already met actin filaments, one of the three types of filaments that compose the cytoskeleton. Actin filaments, shown in Figure 1.5, are themselves polymers composed of monomers of actin proteins. These actin monomers bind together to form long twisted chains that are about 7 nm in diameter. Individual actin molecules, as suggested by Figure 1.5(B) and 1.5(C), are asymmetric. Thus, when many actin monomers are bound to one another to create a filament, it is clear that both ends of the filament are structurally distinct—the actin filament is polarized, with one side referred to as the plus end, and the other, as the minus end. Actin filaments are quite flexible, and form together in networks and bundles to create strong sheets or fibers. In fact, it is quite rare to find individual actin filaments on their own. Actin filaments, and thus actin networks, are made dynamic by the particular way in which

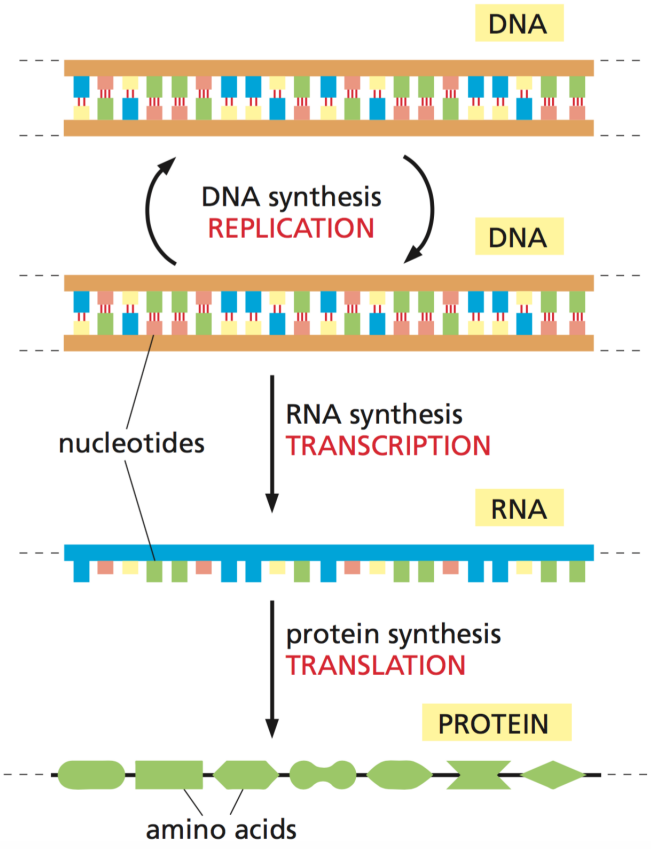

Figure 1.4: **The Central Dogma of molecular biology, or how DNA leads to proteins.** Genetic information is stored in DNA, which self-replicates at division. Sequences of DNA called genes are used to synthesize corresponding RNA molecules in a process called transcription. These RNA molecules are then, in a process called translation, used to synthesize a specific protein, corresponding to the transcribed gene. Image reprinted from [1].

the filaments assemble and disassemble [1].

Actin monomers can be added onto both the plus and minus ends. However, actin monomers bind onto the plus end a good deal faster than on the minus end. The bonds that these actin monomers form with one another are inherently unstable, and it is relatively easy for actin to fall off either end of an individual filament. This occurs because actin monomers have bound to them a molecule called ATP. As shown in Figure 1.6, when ATP reacts with water, it loses a phosphate group and releases usable energy, in the process getting converted to ADP. Once this conversion takes place, the strength between individual actin monomers weakens, and the rate at which the filament spontaneously disassembles increases [29].

When in solutions with high concentrations of actin monomers, actin filaments polymerize quickly. When in solutions with low concentrations, they depolymerize rapidly. There exists, however, a sweet spot between these two extremes, when an actin filament undergoes a process called treadmilling, illustrated in Figure 1.7, where

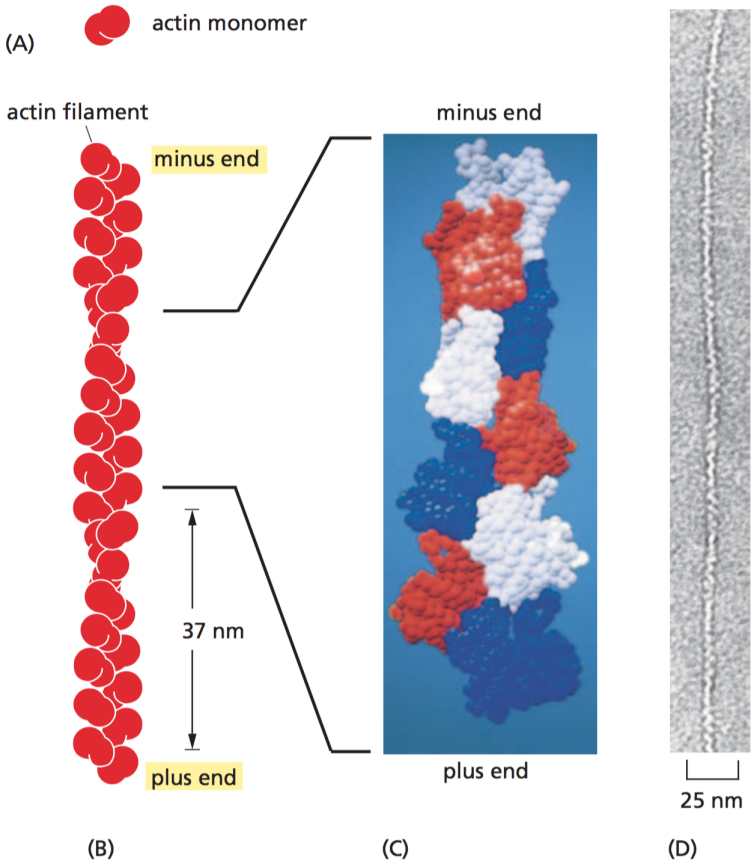

Figure 1.5: **Actin forms long, threadlike filaments.** (A) The actin monomer is made of two proteins bound to each other with a cleft in the middle, where ATP or ADP can bind. (B) The actin filament forms when these monomers bind to one another, end to end, creating a helical polymer that twists completely across about 37 nm. Actin filaments are also polarized, with a plus and minus end, an inherent consequence of the actin monomer's asymmetry. (C) A view showing each individual protein in a different color to emphasize their close, tight interactions. (D) An image of actin taken from an electron microscope. Image reprinted from [1].

actin adds onto the plus end at a rate equal to that with which actin dissociates with the minus end. As a result, the actin filament retains a uniform length [30].

In the cytosol are a collection of actin-binding proteins, many of which prevent or promote the growth of actin. Normal concentrations of actin monomers in the cell are such that actin filaments, left by themselves, would grow at rates and to lengths that would be deleterious, or even fatal, to the cell. These actin-binding proteins, among many other functions, regulate actin filament growth [31].

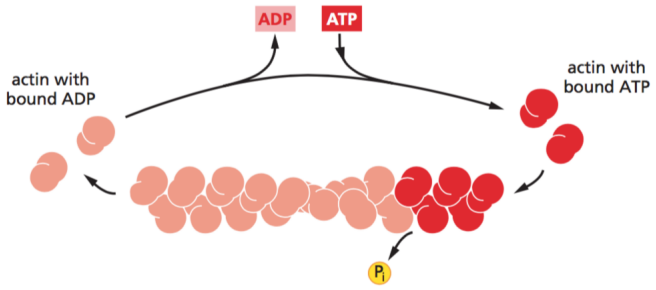

Figure 1.6: **Hydrolysis of ATP causes actin to destabilize.** Actin monomers compartmentalize a single molecule of ATP. Soon after actin filaments form, these ATP molecules hydrolyze into ADP, making them less stable and prone to disassembly. This ensures that actin does not polymerize overmuch, and thus does not distort the cell's shape or interfere with its internal processes. Image reprinted from [1].

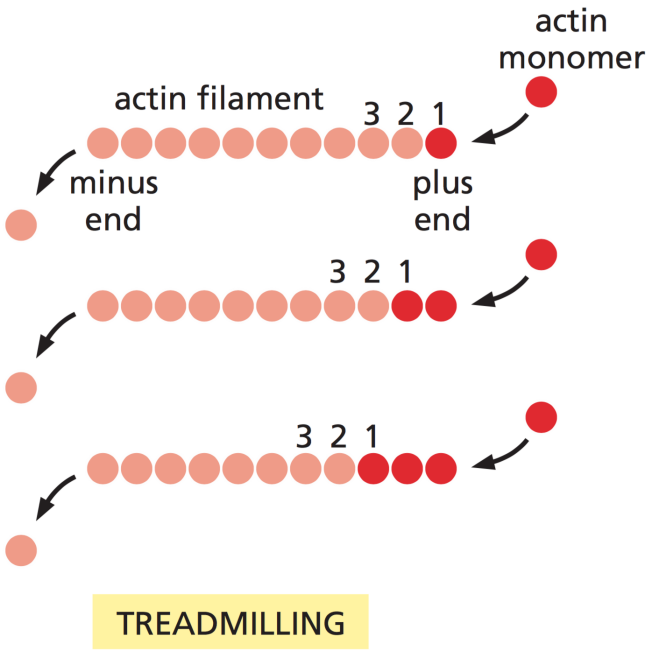

Figure 1.7: **Treadmilling serves to regulate the length of actin filaments.** This occurs when actin monomers polymerize with the plus end of the filament at the same rate that they depolymerize with the minus end, maintaining effectively a fixed length for the filament. Image reprinted from [1].

1.2.2 Myosin motors generate force

Perhaps the most interesting, and certainly the most studied, of all actin-binding proteins is a family of molecular motors called myosin. Myosin proteins all have a head, neck, and tail domain. (A domain is simply a part of a protein that can exist

and function independently of the rest of the protein.) The head domain is the part of the protein that binds to the actin, and, powered by ATP hydrolysis, creates forces that cause it to walk from the plus to the minus end of the actin filament. The neck domain links the head and tail domains, and behaves like a lever to communicate the force generated at the head domain elsewhere along the protein. Finally, the tail domain connects either to molecular cargo or to more myosin, bound together in rod-like fashion. Thus, the tail domain often acts as a cross-linker between multiple actin filaments, transmitting forces between them [1].

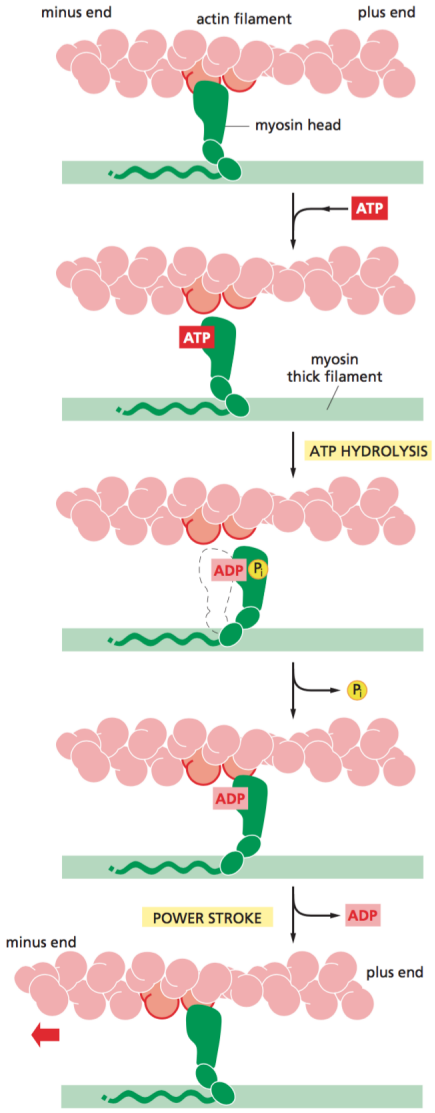

Figure 1.8: **The process by which myosin II walks along actin and generates force.** First, myosin attaches to actin. Then, once bound to ATP, myosin briefly unclutches actin, cocks itself forward (with the ATP losing a phosphate group in the act), and grips actin a small distance further down the filament. Then, with the release of ADP, the myosin tail is dragged forward. Image reprinted from [1].

The particular myosin that is most pertinent to the work presented here is myosin II, shown in Figure 1.8, which is special in that it has two heads, and that the neck domain creates a significant angle between the head and tail domains. This is the motor protein implicated in muscle contraction in muscle cells, but the discussion here will focus more on its very important role in non-muscle cells. Indeed, cell contractility, without which a cell would never be able to migrate, depends fundamentally on the role myosin II plays in cross-linking actin filaments. These myosin II motors grab onto one actin filament via the tail domain, and then walk in lockstep along another actin filament with the head domain. The force thus generated by myosin is leveraged by the actin filaments, which cause the cell to stretch, deform, or protrude [32].

1.2.3 Integrins bind to ECM

Actin filaments, which are so central to the dynamic, mechanical behavior of cells, are crucially linked to the outside of a cell by way of special proteins called integrins. Shown in Figure 1.9, integrins, which are embedded in the cell membrane and thus bridge the inside to the outside of the cell, latch onto the ECM at one end and the cytoskeleton at the other. Once attached to the ECM, they involve themselves in chemical signaling pathways within the interior of the cell that communicate information about the strength and composition of the underlying substrate. From the perspective of this thesis, integrins are the fundamental link between the cell and its environment, acting like a cellular sensing organ to survey the immediate surroundings of the cell membrane [33, 34]. Integrins also play a major role in the tissue development of complex, multicellular organisms. Multicellularity simply is not possible without cells first having the ability to attach to the ECM. If integrins were removed from the cells in an embryo, there would be no hope of tissues ever forming [35].

Once integrins bind to the ECM, large macromolecular complexes called focal adhesions, which include bundles of additional integrins, form at those sites near the cell's surface. To be precise, the signaling pathways discussed earlier are triggered not by the integrins alone, but also by other molecules associated with the focal adhesion complex [36].

1.3 Drosophila Melanogaster is our Model Organism of Choice

In order to study the cellular components and processes discussed above, we are careful to choose a convenient "model organism." The logic behind model organisms is simple. Since all organisms have descended from a single ancestor, the study of one organism can greatly enhance our understanding of many others. *Drosophila*, the common fruit fly shown in Figure 1.10, has been highly important in studying multicellular development, a point of interest for this thesis, in animals. Many of the genes responsible for *Drosophila* development, for example, are very similar to those

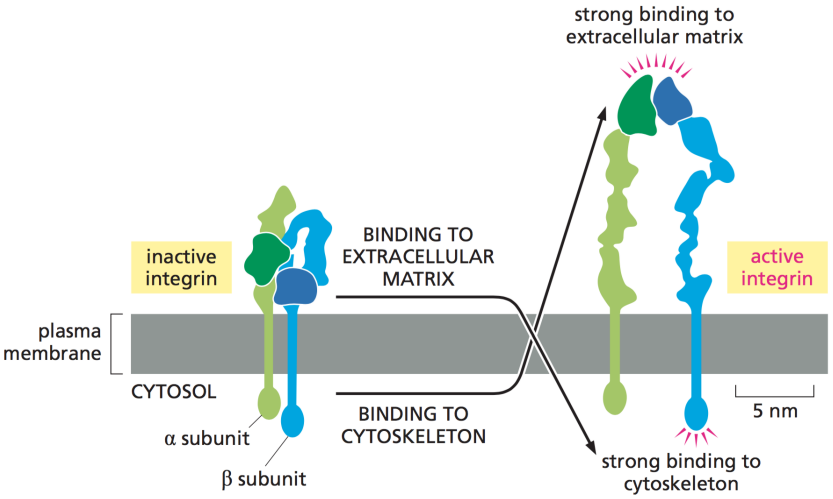

Figure 1.9: **Integrins consist of α and β subunits.** They can exist in an active conformation, where they bind strongly both to the ECM and to the cytoskeleton, and an inactive conformation, where they are not bound to either. Image reprinted from [1].

in human development. The utility of *Drosophila* as a model organism centers on the fact that it is very easy to observe the large-scale biological manifestations, or phenotypes, of mutations induced in its genome. Furthermore, it takes a fairly short time for the *Drosophila* embryo to develop, so many generations of the organism can be studied in relatively small periods of time [1]. Below, I introduce two types of cells that I will later use to test TFM.

1.3.1 Imaginal discs are thin sacs of cells from which certain organs develop

In the *Drosophila* fly larva, little pouches of cells called imaginal discs form around the animal body, and proliferate until they grow significantly in size. Once the fly pupates, the imaginal discs take the next step in development and form all the structures illustrated in Figure 1.11. For reasons largely unknown to us, the imaginal discs, when removed from the larva and allowed to proliferate separately, grow exactly to the size that they would normally. This feature—the fact that the size of the developing disc is regulated by its own devices—has made it a fascinating subject of study, and a legitimate technique by which to observe this stage of development *in vitro* [1, 37, 38]. One of the two cell types made available to me during my thesis work, known as the D25 cell line, was extracted, during the larval stage, from the particular imaginal discs implicated in *Drosophila* wing development. We will return to these cells and the topic of imaginal disc development in Chapter 4.

Figure 1.10: ***Drosophila melanogaster*, the common fruit fly, is a widely used model organism.** *Drosophila* is highly useful in visualizing phenotypes caused by mutations induced in the fly's genome. Because the developmental processes and stages of the *Drosophila* embryo have been so thoroughly detailed, developmental cell biologists often choose to study *Drosophila* cell lines. Image reprinted from [1].

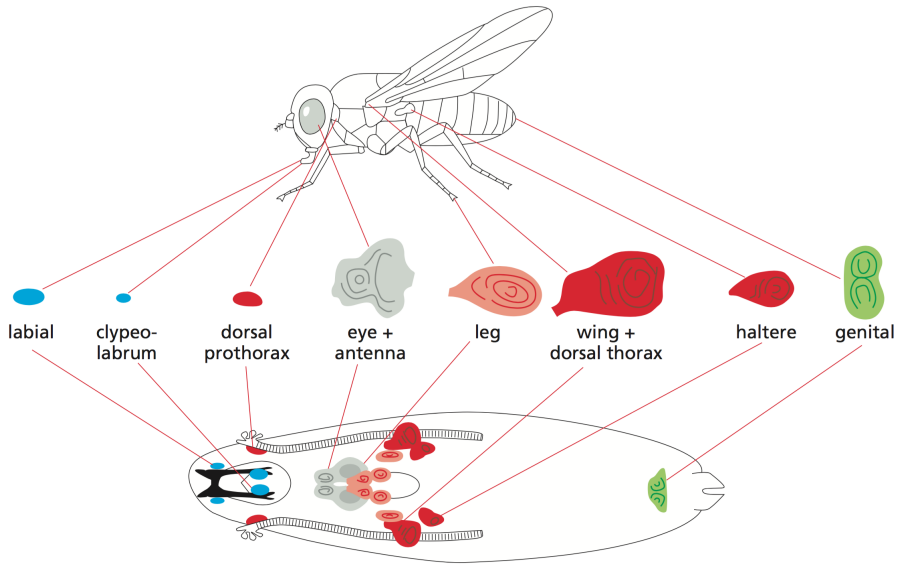

Figure 1.11: **Imaginal discs belonging to the *Drosophila* larva, and their corresponding organs in a mature, fully developed fly.** Image reprinted from [1].

1.3.2 Ras oncogene can make non-cancerous cells cancerous

The second cell type made available to me for my experiments was from a *Drosophila* cell line in which activated Ras, a known oncogene, was upregulated. Activated Ras oncogenes are well known to stimulate rapid, uncontrolled divisions in non-cancerous cells. Ras can be found in some mutated form in roughly 30% of human cancers, and is known to be a significant player in pathways leading to invasion and metastasis [1, 39]. The particular cell that I used is known as RasV12, referring to the fact that the twelfth amino acid in the Ras protein sequence has been mutated. These cells, as will be discussed in the next section, serve to showcase the aberrant contractile properties of cancerous cells. We will return to RasV12 cells in Chapter 4.

1.4 ECM Regulates Mechanotransduction

Mechanotransduction refers to any process in which a cell exhibits a chemical response to a mechanical force. The forces a cell encounters at the cell-ECM boundary are the ones of interest in my thesis. As discussed above, the mechanotransduction apparatus at the cell-matrix level, connecting the inside of a cell to the substratum over which it crawls, consists primarily of an ECM-integrin-cytoskeleton linkage [40].

The cell can increase the strength of its adhesions to ECM by enlarging the number of integrins present at the focal adhesion site, or by recruiting special cytoskeletal proteins that buttress the integrin-ECM bond. It has also been found that cells respond to integrin-mediated forces by remodeling the ECM itself. For example, when fibronectin binds to an integrin, the actin-myosin network pulls on the fibronectin filaments, quite literally prying them apart to reveal more ECM domains to which integrins can bind [40].

Cells exert higher traction forces on stiffer substrates than on softer substrates. When cells exert high traction forces, the actin stress fibers and focal adhesions are found to be tough and robust. When they exert low traction forces, studies have found that the actin stress fibers and focal adhesions are significantly less well developed. While this may seem obvious, the molecular mechanisms that enable this force-sensing behavior are, by and large, unknown. Nevertheless, this mysterious, metaphorical cellular sensory organ is highly correlated with critical processes in development and disease [40]. Below I discuss the two specific cases of mechanotransduction in action.

1.4.1 Mechanotransduction is crucial to embryonic development

The process of measuring mechanical stiffnesses during early embryonic development *in vivo* is extremely difficult. What few measurements that have been carried out consistently point to an excessively soft environment, typically less than 20 Pa. As the embryo continues to develop, these stiffnesses increase by several orders of magnitude. Adult tissues have been measured to have stiffnesses up to 310 MPa [6].

Most studies of cells take place on plastic or glass cultures. Needless to say, these

stiff materials are a far cry from the stiffnesses cells are likely to encounter *in vivo*. Consequently, studies where stem cells were plated on substrates with stiffnesses closer to those found in a developing organism showed remarkable findings. For example, a certain type of stem cell plated on a very soft substrate, roughly the stiffness of brain tissue, was found to express genes at rates suggestive of neuronal differentiation. Those same cells plated on intermediately stiff substrates, similar to the stiffness found in the environs of striated muscle, differentiated into progenitors of muscle cells. Finally, when these cells were plated on very stiff substrates mimicking bone, they were observed to differentiate just as bones cells would [6]. While studies like these have given highly credible evidence of the link between substrate stiffness and cell differentiation, far less studied has been whether a similar correlation can be drawn between substrate stiffness and morphogenesis. This is an area in need of active research. Morphogenesis, in the context of multicellular development, is primarily an act of collective cell migration. Given how tightly controlled ECM stiffness has been shown to be while cells differentiate, it seems likely that the highly coordinated, highly precise migration and positioning observed during morphogenesis also relies on local stiffnesses of ECM [41, 42]. As will be discussed in Chapter 4, we tested this hypothesis by plating our D25 cells on gel stiffnesses differing by two orders of magnitude.

1.4.2 Invasion in cancer is analogous to morphogenesis

Cancer invasion can be seen as the cancer's way of hijacking morphogenesis in order to spread malignancy across an animal body. Just as morphogenesis describes the migration and colony-building behavior of normal embryonic cells, so tumor cells do the same once cells turn invasive and break off from the primary tumor. In more detail, when normal cells differentiate and come together to form tissues, they do so by forming boundaries and linking together via cell-cell adhesions that are mediated by special proteins. With invasive cancer cells, those proteins are downregulated, and the forces the cell exerts at the cell-matrix boundary become far greater than those that exist between adjacent cells. As a result, the cancer cells break free from their colony and spread, forming metastases wherever they successfully settle [43, 44].

Another important feature of morphogenesis in embryonic cells is the presence of metalloproteinases. These enzymes digest the ECM and carve out a trail via which the cell can reach its target. Once the embryonic cell finds its tissue destination, these proteins are deactivated [45]. In invasive cancer cells, however, the transcription of these proteins is upregulated, equipping the cells with the deadly ability to break free from their surrounding tissues and any protective barriers. Once these metalloproteinases present themselves in the cells that comprise a tumor, invasion and metastasis almost becomes inevitable [46, 47].

Cancer, through this lens, is development in reverse. It appropriates the same tools that breathe life into the developing embryos, but uses them to envelop the organism with death. Cancer, then, is mechanotransduction gone awry. The same methods and techniques we employ to test the morphogenetic potential of cells in a developing embryo can, in turn, be used to test the metastatic potential of cancer cells

[15, 48, 49]. As will be discussed in Chapter 4, our own experience with cancerous RasV12 cells, which formed strong adhesions on even the softest substrates, lends strong evidence toward this view.

Chapter 2

The Physical Theory

In this chapter, I outline the statistical and physical ideas that underlie traction force microscopy. To recapitulate, traction force microscopy requires us to fabricate elastic, deformable gels, in which fluorescent beads have been uniformly embedded. These gels are then coupled to ECM, so that a cell migrating overhead attaches to the gel, deforming the substrate as it crawls from one point to another. By taking images of the gel before and after the cell crawls, we can use statistical methods to track the displacements of the beads between the frames. It should be stated at the outset that the statistical technique we use is, with few adjustments, that described in [25]. Then, using elasticity theory, and treating the gel as a three-dimensional springy material, we can calculate the forces that caused the beads to move. Here too, we have borrowed heavily from the work of others, this time from the protocol outlined in [50]. Finally, we can create a vector field of these forces, yielding a quantitative profile of the dynamic behavior of the cell over a given time-frame.[1]

2.1 Cross-Correlation Tracks Bead Movements

The wave nature of light implies that a microscope—constrained by the diffraction limit—cannot image a point source of light as it really exists. Instead, the light will be diffracted, and will be imaged as a series of concentric, glowing halos called an Airy disc, shown in Figure 2.1. This spread of light, which appears on any image of a point source of light, is called the point spread function, as simulated in Figure 2.2. This prevents us from isolating a single pair of coordinates that represent, say, a 100 nanometer fluorescent bead. In order to track the position of a bead, however, we need to determine the position of an individual particle. The statistical technique described here, cross-correlation, allows us to formulate a very good estimate of the center of each particle, and consequently to accurately track its movement.

Shown in Figure 2.3 are a number of fluorescent beads that underlie a cell. While physically the beads look something like that shown in Figure 2.4A, if we were to

[1]The codes we used to cross-correlate and resolve the force vectors were our own adaptations of two codes from Eric Dufresne's group at Yale: the IDL Particle Tracker, and the traction stress calculator contained in the supplementary documents of [50].

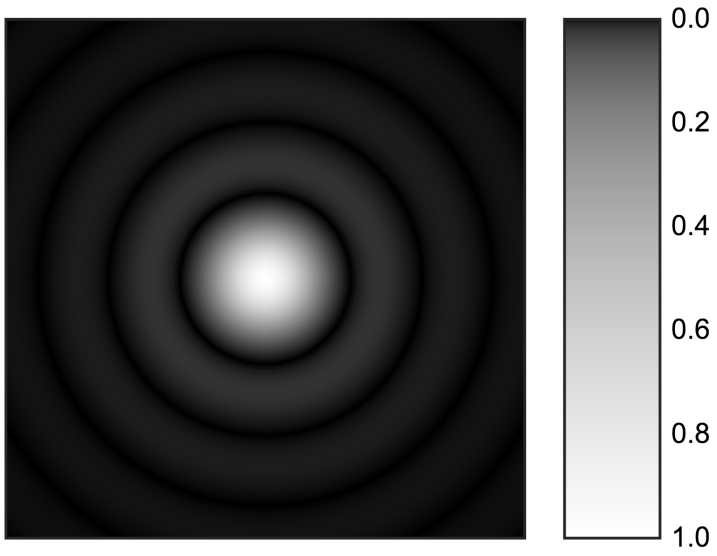

Figure 2.1: **Simulated 2-D Airy disc pattern.** This plot shows the diffraction due to a point source of light.

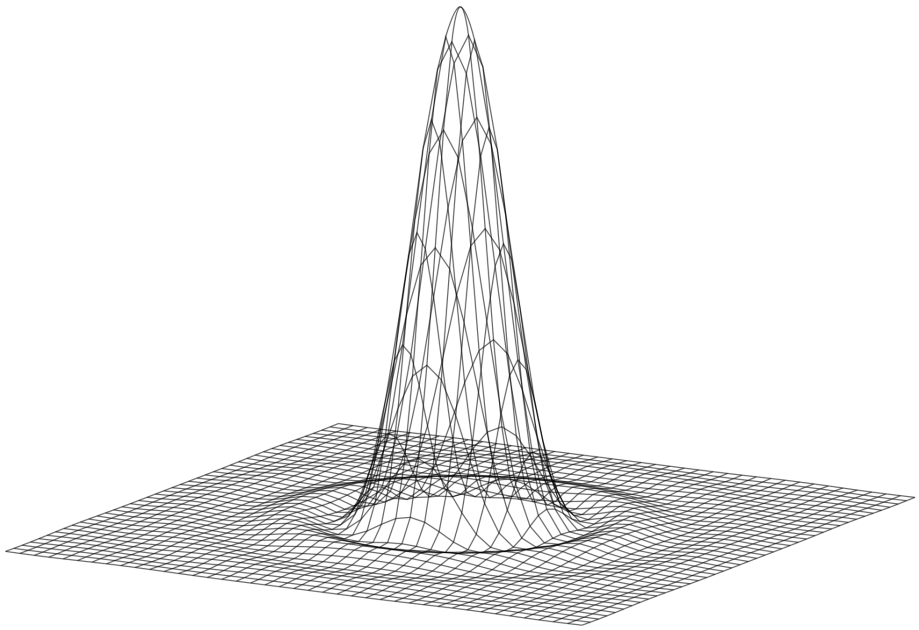

Figure 2.2: **Simulated 3-D intensity plot of the Airy disc formation.**

zoom in on a digitized image taken with a standard microscope, the bead would appear more like the pixelated blob shown in Figure 2.4B. If we have many beads distributed throughout the gel, an image of the bead that is, say, $2n + 1$ pixels in width and height, can be mathematically represented by a two-dimensional function $I(i, j)$. This function quantifies the relative intensity of each bead over the domain

$$-n \leq i, j \leq n. \tag{2.1}$$

Each bead will appear as a circular distribution of intensity, at its edges dropping off to an intensity of zero, where the background is black. Thus, as the bead moves, the entire circular intensity distribution should translate along the domain of $I(i, j)$. In order to track this movement, we cannot simply track the brightest pixel of the distribution—for one, the distribution given by an actual microscope would likely be much broader than that shown in Figure 2.4B. Thus, in many cases, a large portion of the surface of a bead might digitally register with a set of nearly equal intensities. And so, when the bead is displaced, there may be several points on the bead whose pixels momentarily register as the brightest, and such an algorithm would think that the center of the bead is hopping about erratically. We need a better approach.

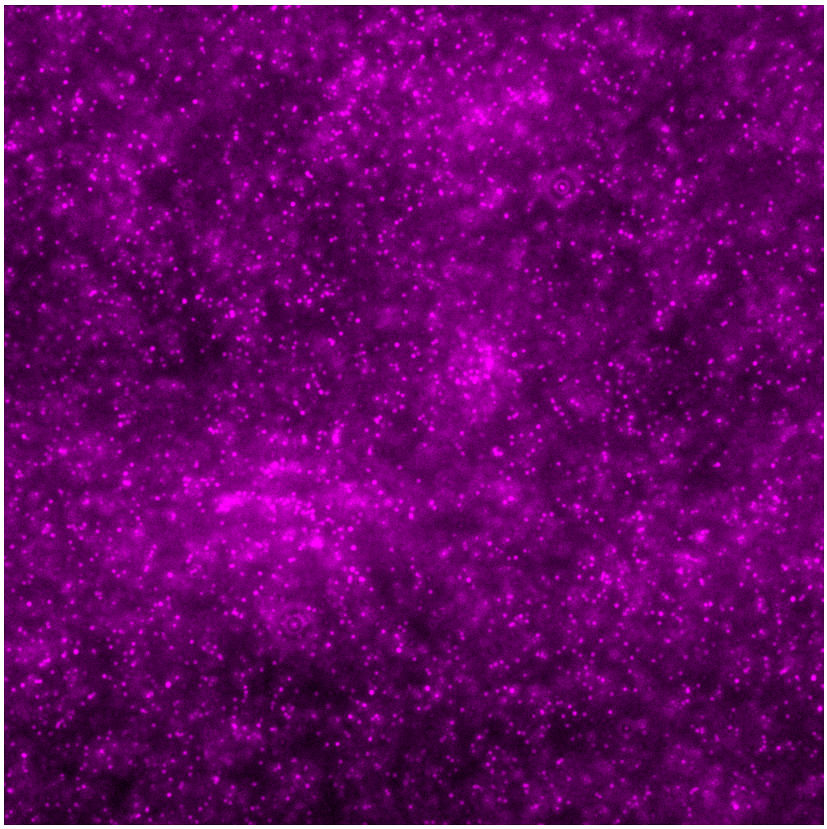

Figure 2.3: **A typical image of** 100 nm **far red fluorescent beads embedded in a gel.** This was taken with an epifluorescence microscope.

The image correlation method we end up using is remarkably precise, and can locate the center of a bead to an accuracy smaller than the width of an individual pixel. In this method, we begin to calculate the translation of the intensity distribution by defining a template image $K(i, j)$, which is calculated from the theoretical distribution that an actual bead of a given size would represent. The template image, shown in Figure 2.4C, is $2m+1$ pixels in width and height, where $m < n$. We then correlate the

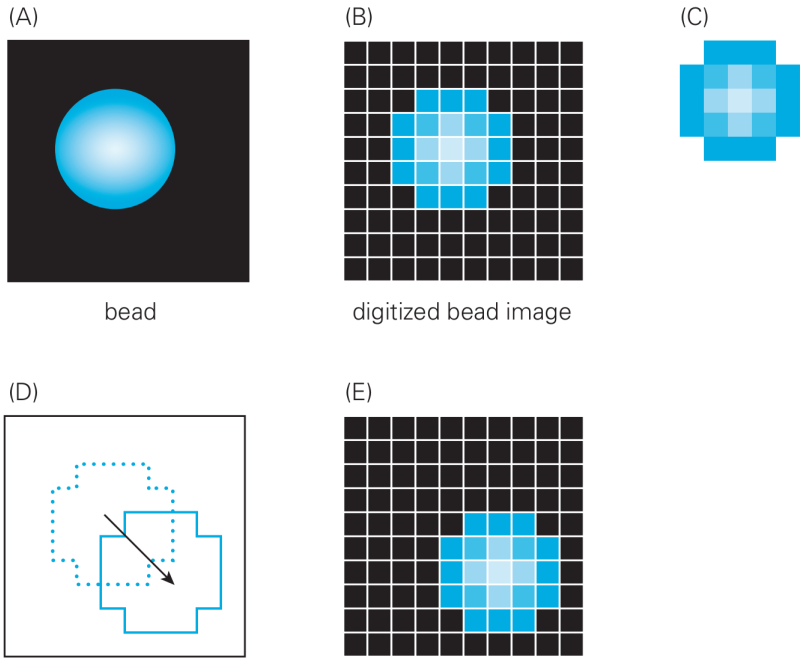

Figure 2.4: **Cross-correlation tracks the digitized images of a moving bead.** (A) An idealized bead, with an increased brightness toward its center. (B) The picture of the same bead once digitized. In reality, it would not look nearly so neat, nor the center be so clearly defined. (C) A template image of a bead. (D) The translation of a bead, treated as though a rigid body. (E) The translated, digitized image of a bead. Again, in reality, the bead would look far less neat, and its points of brightness would be seen to fluctuate. Image reprinted from [25].

differences in distributions from this theoretical, template image, with those from the measured distributions represented by $I(i,j)$. We calculate this statistical correlation, $C(i,j)$, by way of a matrix convolution of I and K, such that

$$C(i,j) = \sum_{x=-m}^{m} \sum_{y=-m}^{m} I(i+x, j+y)K(x,y). \tag{2.2}$$

$C(i,j)$, known as the cross-correlation field, measures the similarity between the intensity patterns given by I and K at a point (i,j). Calculating the statistically most likely location of the bead is simply a matter of finding the position (i,j) that maximizes $C(i,j)$. If the bead has been displaced as shown in Figure 2.4E, then finding the displacement requires only that we subtract the position (i',j'), from the after image, from the position (i,j), from the before image, to get a displacement vector like that in Figure 2.4D. We can even improve this calculation, bringing it to sub-pixel accuracy, by calculating the centroid of $C(i,j)$, with the improved positions (i_c, j_c). In theory, if the bead's initial position was at the origin, the coordinates for its centroid would be given by

$$i_c = \frac{\sum_{i,j} iC(i,j)}{\sum_{i,j} C(i,j)}, j_c = \frac{\sum_{i,j} jC(i,j)}{\sum_{i,j} C(i,j)}. \tag{2.3}$$

2.2 Elasticity Theory Can Resolve Forces from Displacements

Once we have an accurate set of displacement vectors, the next step is to calculate the forces that brought about those displacements. By forming our gels out of an isotropic material like polyacrylamide, we can use elasticity theory to relate the forces to the displacements in a fashion analogous to calculating the force produced by a spring, F, displaced a distance x, given by Hooke's law, $F = -kx$, where k is a constant describing the elasticity of the spring. In our case, we regard a patch of material, such as that shown in Figure 2.5, displaced by a distance u due to a lateral force F, tugging laterally at the top surface of the gel. The bottom of the gel we assume to be anchored to a rigid substrate. The displacement of that patch caused by the force F will depend on a number of properties inherent in the material of the gel—its thickness, stiffness, and compressibility. In reality, there is no discrete force like F exerted laterally at a given point on the gel. Rather, there is a continuous distribution of force, which we describe via a traction stress, σ_{iz}. The traction stress measures the force per area exerted laterally on the surface of the gel.

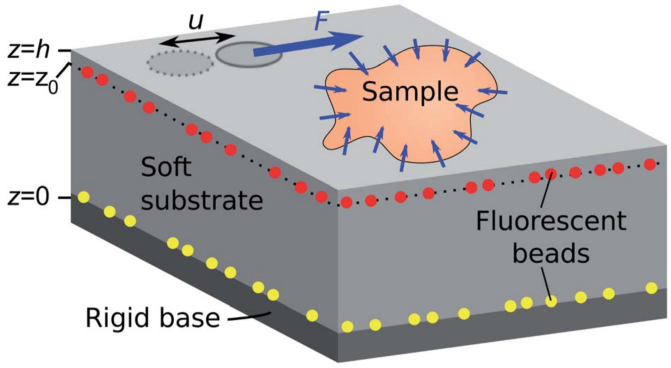

Figure 2.5: **Schematic for gel.** Fluorescent beads of interest are shown to be very near z-plane plane of cell. Image reprinted from [50].

Assuming the gel is a linear-elastic solid, we can relate the stresses $\boldsymbol{\sigma}(\boldsymbol{x})$ to the displacements $\boldsymbol{u}(\boldsymbol{x})$ with the tensorial form of Hooke's law,

$$\boldsymbol{\sigma} = \frac{E}{1+\nu}\left(\frac{1}{2}(\nabla \mathbf{u} + \nabla \mathbf{u}^{\intercal}) + \frac{\nu \nabla \cdot \mathbf{u}}{1-2\nu}\mathbf{I}\right), \tag{2.4}$$

where ν is Poisson's ratio, E is the Young's modulus, and $\mathbf{I}$ is the identity tensor. Under the condition of mechanical equilibrium, $\nabla \cdot \boldsymbol{\sigma} = 0$, Eqn. 2.4 reduces to the

form

$$(1-2\nu)\nabla^2\mathbf{u} + \nu\nabla(\nabla\cdot\mathbf{u}) = 0. \tag{2.5}$$

We solve this equation by applying the boundary conditions for our specific case. To begin with, the gel is firmly attached to the coverslip below, at $z = 0$, but it is free to be tugged and pushed at the surface in contact with the cell, at $z = h$. By focusing the microscope on the the beads present very near the top surface of the gel, we can thus treat the bead displacements as displacements taking place on the top surface of the gel, so we will assume the beads are at position $z = z_0 = h$. Defining $\mathbf{u}^*(x, y)$ to be the deformations at the gel surface, we can state the following boundary conditions:

$$\mathbf{u}(z = h) = \mathbf{u}^*(x, y), \quad \mathbf{u}(z = 0) = 0. \tag{2.6}$$

We can now solve Eqn. 2.5 by applying Fourier transforms in x and y. This results in an ordinary differential equation in terms of the Fourier transform, $\hat{\mathbf{u}}(k_x, k_y, z)$, of $\mathbf{u}$, where k_x and k_y are the wavenumbers in x and y. When this ODE is evaluated at the gel surface, we reach a relation between $\hat{\mathbf{u}}$ and the Fourier transform of the traction stresses, $\hat{\boldsymbol{\sigma}}$,

$$\hat{\sigma_{iz}}(k_x, k_y, z = h) = Q_{ij}(k_x, k_y; h)\hat{u_j}(k_x, k_y, z = h), \tag{2.7}$$

where repeated indices are summed. The matrix for $\mathbf{Q}$ is too cumbersome and unwieldy for this section, but can be found in [50]. Thus, all in all, the procedure discussed above can be summarized in four steps.

1. Calculate the Fourier transform of the displacements in the plane $z = h$.
2. Find the $\mathbf{Q}$ matrix for each pair of wavenumbers (k_x, k_y).
3. Calculate the Fourier transform of the traction stresses by applying the $\mathbf{Q}$ matrix to the displacements for all k values.
4. Perform an inverse Fourier transform to determine the traction stresses.

That's it—we need only to repeatedly run our data through this algorithm to systematically calculate the traction stresses at the gel surface. If all goes well, the result should resemble that shown in Figure 2.6.

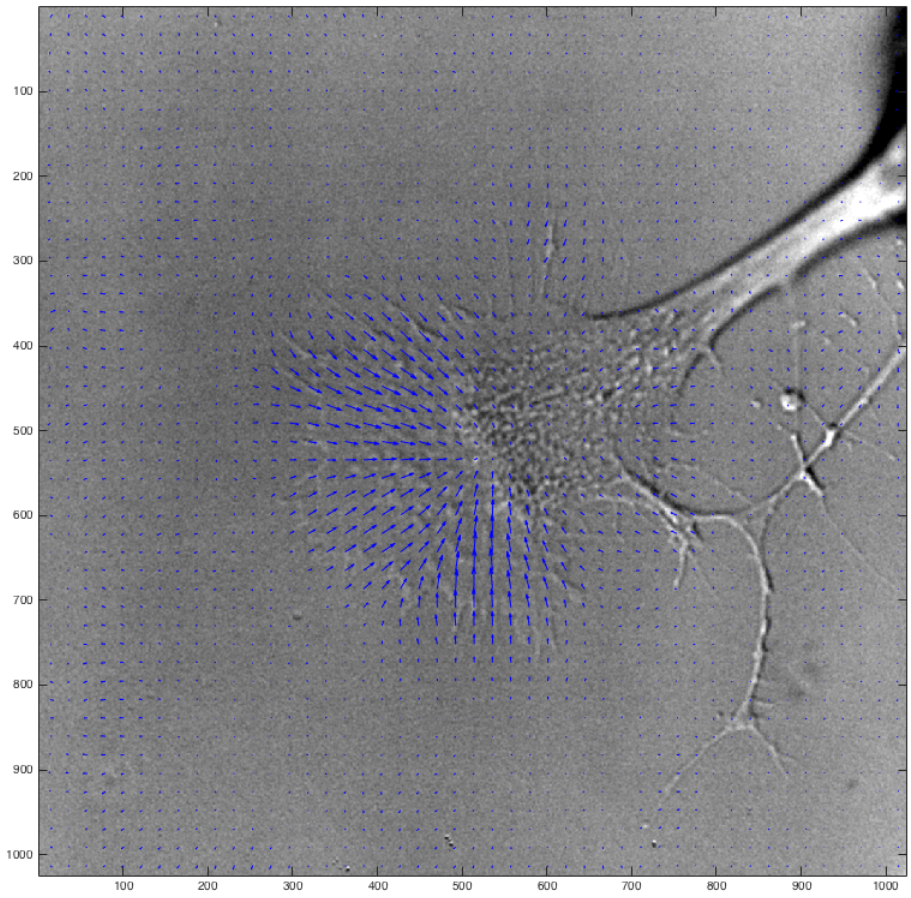

Figure 2.6: **Traction force field plot.** This vector field was calculated with sample data from [50].

Chapter 3

Experimental Design

3.1 Forming Compliant Matrices and Imaging

The procedure for creating smooth, compliant matrices embedded with beads is difficult and includes a number of tricky, time-sensitive steps. It was only after many missteps and misfires that I finally saw the bead movement I was hoping to observe and capture. The first section of this chapter owes a very heavy debt to a procedure formulated by Margaret Gardel's group at the University of Chicago [51]. The protocol below is our adaptation of Gardel's protocol to the epifluorescence microscope and cells available in the Applewhite lab.

3.1.1 Activating the coverslips

The first step of our procedure is to wash the coverslips. We always began by arranging the coverslips in a stainless steel coverslip holder (Electron Microscopy Sciences, 72239-04), which we then immersed in etching solution (120 g KOH in 120 mL H_2O + 880 mL isopropanol). We let the coverslips soak in the solution for two or so hours, and then rinsed them in running deionized (DI) water for 15 minutes. We then placed the coverslips (still in the holder) on a hot plate set to 100 °C until most of the moisture on them had evaporated (usually between 3-5 minutes). From here on, and throughout the procedure, we wanted to avoid dust particles from landing on the coverslips; thus, if the coverslips were not in a solution of some sort, they were in a clean glass tub covered loosely with a layer of aluminum foil.

Activating the coverslips, which allows the gel to anchor to the glass, involves a number of very toxic chemicals, so the remaining steps of the protocol were performed in a fumehood. We made sure that at each step our hands were gloved, that we were wearing lab coats, and that our eyes were protected with laboratory goggles. We also made sure there was an abundance of empty waste containers for disposal of washes and Ziploc bags for contaminated gloves. First, we diluted 3-aminopropyltrimethoxysilane (Aldrich, 28, 177-8) in isopropanol to reach a concentration of 2% (2 mL silane/100 mL isopropanol), enough to fill at least a small square dish (roughly 350 mL). We used glass Pasteur pipettes to transfer the 3-aminopropyltrimethoxysilane, a highly reactive chemical. We immersed the coverslip

holder in this solution and allowed the coverslips to soak for 10 minutes while gently stirring on a stir plate. While we waited, we filled up four other square glass dishes with roughly the same quantity of DI water (350 mL) as in the previous solution. After the soak, we transferred the coverslip holder to one dish of DI water, letting it sit for 10 minutes, and rinsing and repeating for each of the other three dishes we filled. For the final wash, we let the coverslips soak for 10 minutes with stirring. Following these steps, we properly disposed of all the amino-silane containing solutions by carefully pouring them into specially labeled waste containers.

Following the final wash, we put the coverslips in an incubator set to 37 °C, where we waited roughly 30-60 minutes for the coverslips to dry. Generally, the coverslips did not fully dry in the incubator, so after removing the coverslip holder we placed it on a hot plate set to 100 °C for 3-5 minutes (again, loosely covered in aluminum foil), until the residue of DI water had evaporated. We then turned off the hot plate and allowed the coverslips to return to room temperature.

Finally, and now back in the fume hood, we immersed the coverslips in 1% by volume glutaraldehyde solution in DI water in a clean glass square dish for 30 minutes with stirring. This step completed the coverslip activation process. As with amino-silane, we performed a series of successive washes in DI water following the glutaraldehyde soak, though this time only three instead of four. We then properly disposed of all the glutaraldehyde containing solutions in specially labeled waste containers. Finally, we allowed the coverslips to dry at room temperature in yet another glass square dish, which we covered in aluminum foil, loosely enough so that it was not airtight but still would prevent dust from getting in. Once here, we could store away our coverslips in a dry, dust-free place for up to 2 months. Every time we needed some coverslips from this collection, we were wary about removing them carefully (to avoid dust), and then immediately re-covering the dish with foil.

3.1.2 Preparing the polyacrylamide gels

This section of the procedure relies on the quantities listed in Table 3.1. It is up to the experimenters to choose the stiffness they want for the experiment at hand, and to follow Table 3.1 accordingly. We will here describe how to make gels on three 8 mm × 22 mm coverslips; others can attempt to work with more, but doing so will make the procedure significantly less manageable during the time-sensitive steps.

We began by making stock solutions by mixing 40% acrylamide (Bio-Rad, 161-0140) and 2% bis-acrylamide (Fisher Scientific, BP1404) according to Table 3.1. The stock solutions should be made in darkened bottles and kept at 4 °C, where they can then be stored and retrieved for a number of years. To make working solutions, we diluted stock solutions, again according to Table 3.1. We degassed the working solution in a vacuum chamber at -25 psi for 20 minutes, which removes oxygen and inhibits polymerization. We then sprayed Rain-X on a microscope slide. Keeping the slide clean, we allowed it to dry for a couple minutes, and then wiped away any excess Rain-X with a separate kimwipe dampened with a single spray of Rain-X. In the fumehood, we cut out a piece of Parafilm and lay the slide upon it, with the side we wanted to work with exposed. Then, we added fluorescent beads (TetraSpeck

Table 3.1: Stock and working solutions for polyacrylamide (PAA) gels. Source: [51].

Stock PAA Solution				
Shear Modulus of PAA Gel (Pa)	**230**	**2833**	**8640**	**16344**
40% Acrylamide (mL)	1.25	3.12	2.34	2.50
2% Bis-Acrylamide (mL)	0.50	0.83	1.88	0.60
Water (mL)	3.25	1.04	0.78	1.90
Total Volume (mL)**:**	5	5	5	5
Working PAA Solution				
Stock Solution Used (Pa)	**230**	**2833**	**8640**	**16344**
Stock Solution Volume (µL)	150	150	200	300
Water (µL)	341.75	341.75	291.75	191.75
Beads (µL)	5	5	5	5
TEMED (µL)	0.75	0.75	0.75	0.75
10% APS (µL)	2.5	2.5	2.5	2.5
Total Volume (µL)**:**	500	500	500	500
Final Acrylamide %	3	7.5	7.5	12
Final Bis-Acrylamide %	0.06	0.1	0.3	0.15

Microspheres, 0.1 µm, fluorescent far red), TEMED (Fisher Scientific, BP 150-20), and APS (Fisher Scientific, BP179) according to the quantities listed in Table 3.1. At this step, time became very limited: we had minutes before the gel began to polymerize. We briskly pipetted up and down to mix the beads. Then we applied three dots of 8 µL of the solution each to the Rain-X treated slide. Each dot was separated by at least 20 mm, leaving enough space between them so that adjacent coverslips should not touch or overlap. We then carefully laid down a single activated coverslip on each dot of solution, and waited, generally about 10 minutes, for the gel to polymerize. Once we could see the coverslip barely begin to lift from its edges off the glass slide, we used a razorblade to remove the coverslips and placed them individually in separate small, sterilized Petri dishes that were filled with DI water. Finally, we covered the Petri dishes and wrapped their sides in Parafilm to prevent contamination.

3.1.3 Coupling ECM to the polyacrylamide gels

There are several methods by which to cross-link ECM to the polyacrylamide gel surface. We used the sulfo-SANPAH method for no other reason than that our guru, Margaret Gardel, uses this method in her lab at the University of Chicago. Alternative coupling methods can be found in [51]. The first step is to prepare working aliquots of sulfo-SANPAH, each with 2 mg of sulfo-SANPAH powder (Pierce, Thermo Scientific, 22589) and 40 µL of dimethyl sulfoxide (DMSO), and then flash-freezing them in liquid nitrogen. These can then be stored at −80 °C. Next, we retrieved our coverslips from the Petri dishes and very quickly (1-2 seconds) spun them down with a benchtop

picofuge that had been fitted with claws (fabricated in the Machine Shop by Jay Ewing) designed to hold the coverslip in place. We then diluted a sulfo-SANPAH aliquot in DI water to a concentration of 2 mg/mL. The moment this dilution took place, we had to act very quickly, since sulfo-SANPAH has a reactivity half-life of roughly 5 minutes at room temperature. We distributed about 200 µL of the diluted sulfo-SANPAH solution evenly across each coverslip, and then exposed them to a UV lamp (8 W, 254 nm, borrowed from the Chemistry Stockroom), holding the lamp a few inches from the coverslips. If successful, the red sulfo-SANPAH color would visibly change to a darker, bronze color. We cut out a strip of Parafilm and transferred three dots of 35 µL of ECM on each. We then dipped each of the coverslips in DI water, very quickly spun them down (again, no more than 1-2 seconds sufficed), and laid each one, gel side down, on each of the dots of ECM. Finally we placed the coverslips, still reacting with the ECM, in a Petri dish, in which we placed a few damp Kimwipes. We then sealed the Petri dish with Parafilm and left it to incubate at 20 °C overnight.

3.1.4 Plating cells and imaging

After the incubation was complete, we melted the contents of a bottle of VALAP (a 1:1:1 mixture of petroleum jelly, lanolin, and paraffin) by placing it on a hot plate set to roughly 120 °C. We then removed the coverslips from the ECM using a sterilized pair of tweezers and placed them, gel side down, on the back of coverslip dishes whose bases had holes cut by the laser cutter found in the Reed machine shop. We sealed the edges of the coverslips by applying fully molten VALAP via the tip of a paintbrush. Looking closely for any exposed edges, we made sure the edges were completely sealed to prevent leakage.

Quickly, so that the gels did not dry, we transferred the dishes to the cell culture hood and added 2 mL of cell media to the inside of each of the dishes. We then added, depending on the density of our cells, anywhere from 100-250 µL of cells, and covered the dishes, placing them in a cell culture incubator.

We waited until the cells attached, which, depending on which cells were tested and the stiffness of the substrate, could take anywhere from hours to days. Once the cells were attached (which could be verified under a light microscope), they were ready for imaging. We placed the dish onto an imaging chamber, and then placed the chamber above the microscope objective and began imaging. In our case, we created movies of the bead displacement by taking snapshots of the beads every 10 seconds, switching between far red epifluorescence and bright field, to image, in turn, the beads and the cell itself.

Chapter 4

Results and Discussion

This thesis is, in the end, a methods thesis. By this I mean, the entire duration of my thesis was spent trying to get the method to work in the first place. It took 63 failed coverslips before we saw any bead movement whatsoever. But when we did finally observe the beads to move, and ran the images through our tracker and traction stress calculator, the results were spectacular. In the next section, I show a number of the beautiful plots we obtained, which give extremely precise dynamic profiles of the mechanical behavior of the cells. Following that section, and for the benefit of future students who wish to pursue these experiments further, I will outline the major mishaps and misadventures that eventually led to our successful run of the experiment.

4.1 It Worked!

We collected many hours of footage, documenting the traction-induced bead movements caused by RasV12 cells. Due to time constraints, we were unable to take TFM to the next level, comparing changes in traction stresses as cells from a given cell line were plated upon a whole range of different gel stiffnesses. This I leave to future students, from both physics and biology, who wish to use TFM to build upon my thesis work. As a result, this section is necessarily light on analysis. The point of my thesis has been to put in the elbow grease to introduce TFM to Reed. The fruits of this effort, more positive than I could have hoped for when I first set out on this project, are shown below in Figures 4.1–4.4, showcasing cells in a wide variety of dynamic situations.

4.2 How We Eventually Saw Bead Movement

I refer affectionately to these setbacks as blunders. In truth, it was these blunders—which drew from me much toil and sweat—that I am most grateful for; they taught me the trials and triumphs that are part and parcel of trying to set up a novel experiment. From no other experience at Reed did I learn so much about the actual *doing* of science. The most trying of these blunders are laid out below in roughly

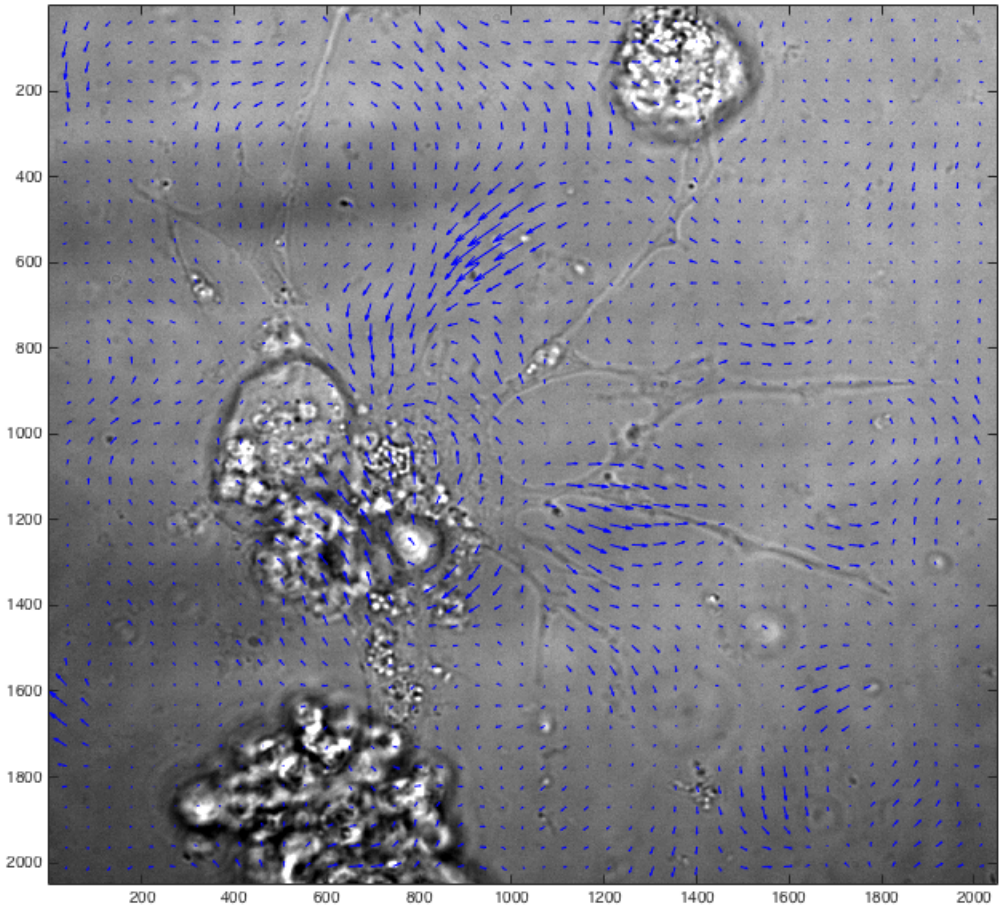

Figure 4.1: Bead displacements were taken 15 seconds apart. The maximum particle displacement was set to 16 pixels. The force vector arrows were scaled by 1.5. The image shows an area of 133 µm × 133 µm. We very clearly see the force vectors align with the highly contractile projections with which the cell is, from above, pulling inwards, and below, pushing outward.

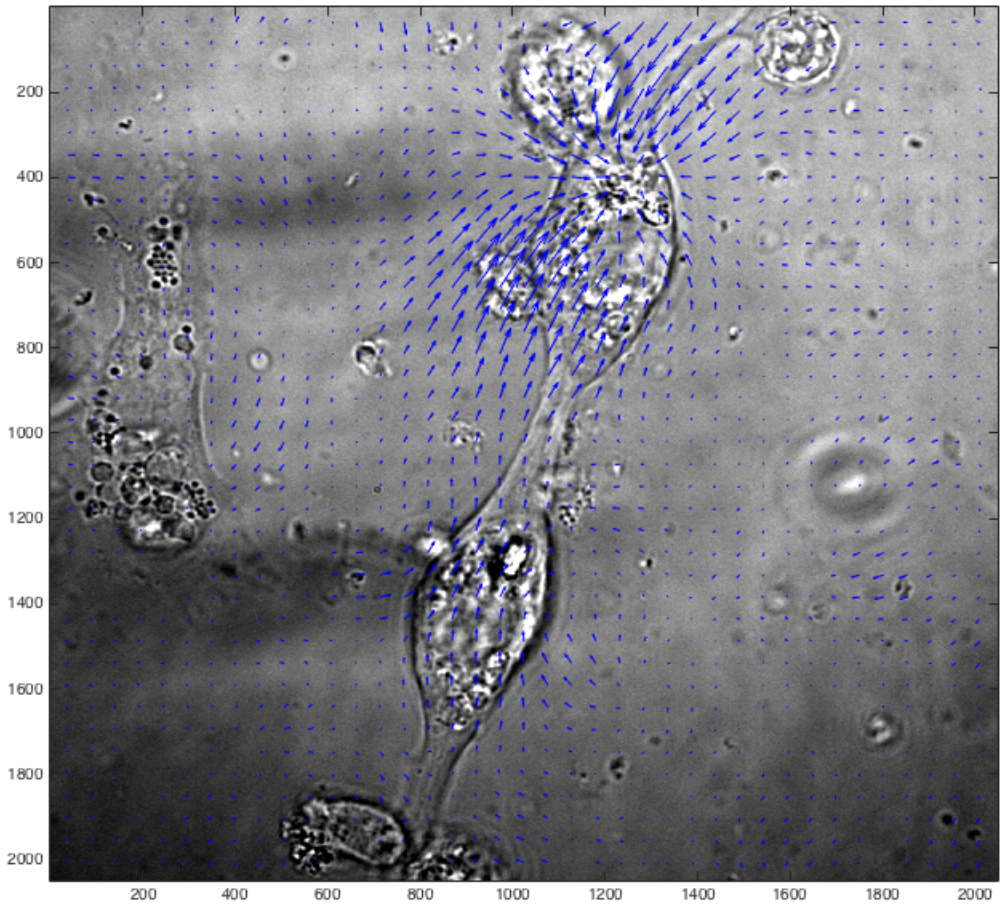

Figure 4.2: Bead displacements were taken 30 seconds apart. The maximum particle displacement was set to 12 pixels. The force vector arrows were scaled by 1.5. The image shows an area of 133 µm × 133 µm.

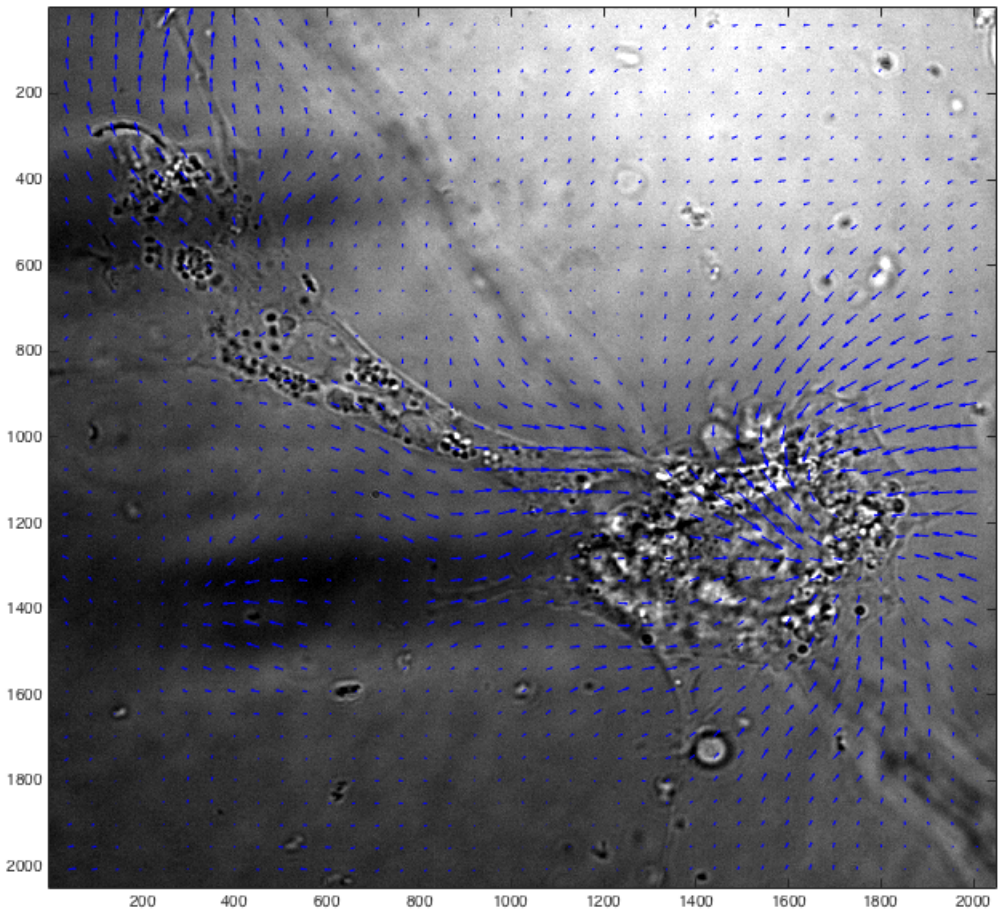

Figure 4.3: Bead displacements were taken 30 seconds apart. The maximum particle displacement was set to 16 pixels. The force vector arrows were scaled by 1.0. The image shows an area of 133 µm × 133 µm.

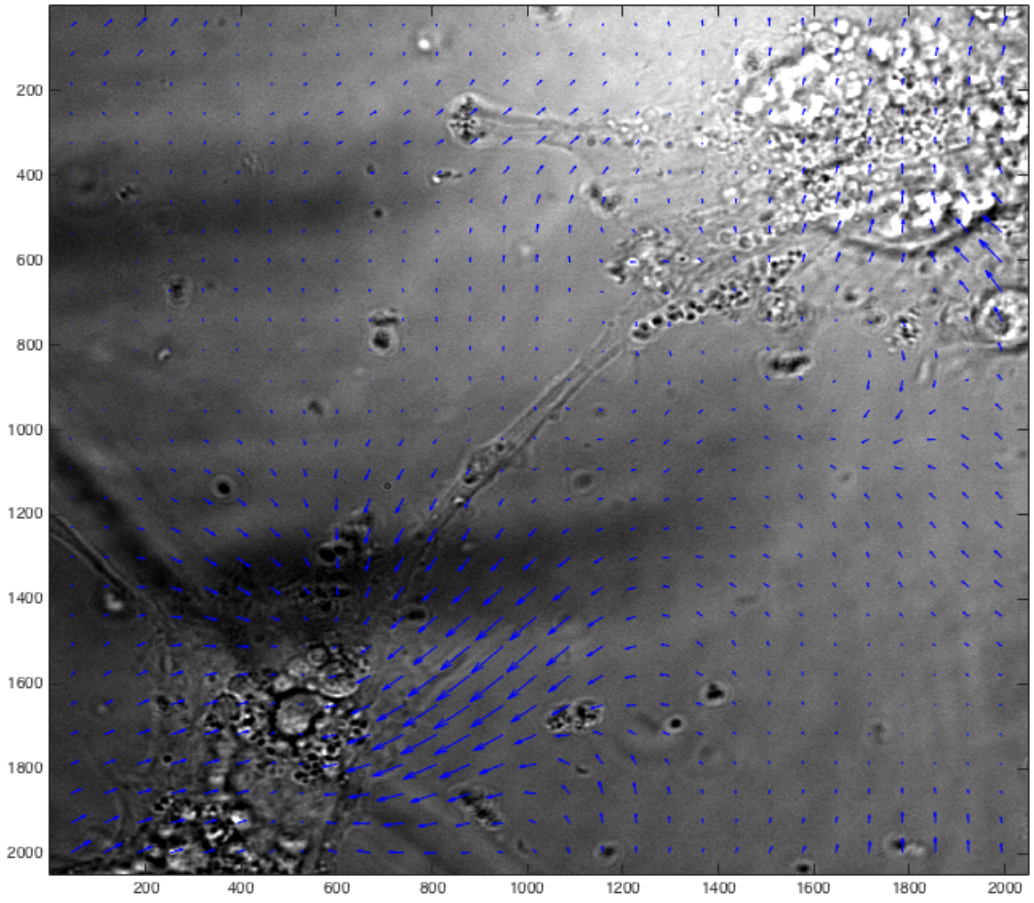

Figure 4.4: Bead displacements were taken 30 seconds apart. The maximum particle displacement was set to 18 pixels. The force vector arrows were scaled by 1.0. The image shows an area of 133 µm × 133 µm.

chronological order.

4.2.1 Sealing the coverslip to the dish

The first problem that we encountered was how to seal the coverslips to the laser-cut dish. Initially we did this by using a syringe to squeeze out a thin layer of vacuum grease around the rim of the dish's aperture. We had to do this step very quickly (within five minutes) to prevent the gel from drying and deforming. Immediately after the seal was made, we transferred the dish to the cell culture hood, where we deposited cell media over the gel to hydrate it (the same media that soon would feed the cells, thus serving two purposes). Inevitably, however, two or so of the three dishes would leak out their media. The gels that were attached to those dishes, whose edges were now wet, were impossible to reattach to the dishes in time without having the gels dry out, because vacuum grease attaches very poorly to a wet surface. Those gels had to be discarded. If we were lucky and one gel survived without leaking, we would quickly plate our cells on the gel. While the cells were attaching—which, depending on the cells used and gel stiffness, could take anywhere from minutes to half a day—there was a good chance that the vacuum grease would fail to keep a good seal, and the cells and media would leak out. This meant that the coverslip had to be discarded. If, on the rare occasion the vacuum grease did keep a good seal, and the cells were able to attach, we immediately fixed the dish to a mounting plate, being careful not to let the grease slide. Even if we were able to image cells, though, this step always felt treacherous, because if the cells and media were to leak, they would destroy the objective on Derek's microscope.

Solution. We finally solved this problem by switching our sealant entirely. VALAP, whose composition is given in the previous chapter, is a waxy substance, far less finicky about wet coverslips and far more robust when dry. Melted over low heat, and applied with a paintbrush, it should be coated around the edges of a coverslip in a thin layer, and care should be taken to ensure there are no holes or small spaces from which media can leak. Once the VALAP is dry, the dish should immediately be transferred to the cell culture hood, the media added, and the cells plated.

4.2.2 Using the right fluorescent beads

The protocol by Margaret Gardel's group says to use blue fluorescent beads when making gels. Thus, we followed its advice and ordered 100 nm blue fluorescent beads. We continued using these beads well into the second semester. During that time we never saw bead movement, but this choice of beads created an even greater problem. The cells themselves could hardly be imaged for more than a few minutes, because the blue light induced in them an early programmed cell death (PCD). PCD is generally characterized by cell shrinkage and blebbing, both of which can be easily visualized. Blebbing in particular involves clearly discernible bulges and protrusions emerging from the plasma membrane, as though the cell were blowing bubbles.

Solution. We initially treated the PCD as an unavoidable nuisance, an inevitable

consequence of shining high intensity light on the cell. This, it turned out, was not the case. Eventually, since we had already bought with money from the Initiative Grant a far red filter for the microscope (to visualize focal adhesions, not beads), we decided to see if the cells would survive longer with 100 nm far red beads, which have excitation/emission peaks at 690/720 nm. When the beads arrived and we used them in our next set of gels, we were very surprised to see that cells seemed, on the whole, unaffected by the excitation light. Even during very long imaging sessions with the same cells, we no longer saw blebbing or cell shrinkage.

4.2.3 Getting the cells to attach

Sometimes during our experiments the cells would attach; sometimes not. The RasV12 cells appeared, by and large, to attach to gels of any stiffness. The D25 imaginal disc cells would rarely attach to any gel, no matter its stiffness. This puzzled us a great deal, especially when we ran out of RasV12 cells and for a period of three weeks tried to make do with D25 cells.

Solution. The problem here, it turns out, has more to do with biology than with experimental design. The cancerous RasV12 cells, as I have argued earlier in my thesis, exert far greater traction stresses than their non-cancerous counterparts would be expected to [24]. Cancer cells, of course, originate from a fully formed tissue. The process of metastasis can be traced to when the cell begins exerting large enough forces that it can physically break away from any ECM or tissue boundaries that block its path to the circulatory system. This, quite likely, is the reason why the Ras cells adhered to any substrate we plated them on.

On the other hand, the D25 cells were removed from the imaginal discs of a developing fly larva. During this stage of development, the cells are in the process of forming a single-cell-thick epithelial sheet. Consequently, the high stiffnesses of ECM generally found near already developed, mature tissues cannot be expected. Presumably, the stiffnesses are as low as those in the early embryo, so close to 20 Pa [6]. However, the softest gel stiffness for which we had a protocol was 230 Pa. Therefore, even with our softest gel, we probably could not simulate the typical conditions that these delicate cells, quite unlike the robust and powerful RasV12 cells, are ideally conditioned to. It may in fact be the case that D25 cells within the developing imaginal disc sac never strongly attach to any ECM scaffold in the first place; that, in order to form the initial epithelial sheet, cell-cell adhesions are far more of a priority than cell-matrix adhesions. If this is the case, then trying to get D25 cells to attach and thereby produce measurable tractions with any of the gel stiffnesses available to us might have been a lost cause all along.

4.2.4 Coupling the ECM to the gel

After we had eliminated all the other variables we could think of, we were unsure where to turn. The gels I fabricated appeared beautifully under the microscope, often better than the gels I saw in TFM papers I was reading. The RasV12 cells were clearly strongly attached to the ECM below. But somehow, the gel remained

unperturbed—the beads simply did not move. I emailed Patrick Oakes, a researcher in Margaret Gardel's group, for advice. After I answered a number of questions he had about our setup, he responded saying that, almost certainly, the problem had to do with the coupling step, where the ECM is chemically bonded to the gel underneath. It turns out that the concentration of ECM protein typically used to coat glass coverslips is roughly 10 µg/µL. The concentration of ECM used when coupling to a gel is 1 mg/µL, a two order of magnitude difference. While this number can be tightly controlled when working with commercially available ECM, where the quantities of protein (for example, fibronectin or collagen) are precisely known, this was far from the case with the ECM we used.

Working Solution. The commercially available ECM for fly cells contains protein that prevents the fly cells from migrating, since *Drosophila* cells are not conventionally used to study migration. Thus, the Applewhite lab harvests its own ECM protein from cell media secreted by migrating cells. Typically, the ECM the lab had been using for the previous year had to be diluted to 1/25th the stock concentration. If we were to follow Patrick's advice, the stock concentration needed to be at least four times as dense with ECM protein.

Derek had entrusted the task of harvesting ECM to a previous thesis student, who botched one step of the complicated protocol by which the ECM is isolated from media, causing the ECM to be more dilute than usual. This was not a problem for anyone else in the lab, but was for me, since I needed high concentrations. Thus, Derek and I spent three days harvesting new ECM stocks, taking great care to prevent mistakes. In the end, the ECM was certainly more concentrated than the previous solution, perhaps twice so. This, however, we could only confirm qualitatively by diluting quantities of the ECM, coating them on glass, and checking if the cells still attached as normal. It was with these new, more concentrated stocks of ECM that we finally succeeded in getting the ECM and gel to couple. Unfortunately, in the 16 coverslips I subsequently made (admittedly hastily, given what little time I had left), we could not get good coupling, and thus never saw the beads move again.

My thoughts on why the experiment continued to fail are simple: the problem is due to poor coupling, and the poor coupling is due to the fact that the concentration of ECM is *still* not dense enough. I am suspicious of whether our normal method of ECM isolation can yield the concentrations we require for good coupling. Likely, unless we switch cell types and thus can purchase commercial ECM of known concentration that does not prevent migration, the first step would be to measure protein concentration with a spectrophotometer. I would have carried this out myself had I not run out of time. If the concentration is near 1 mg/mL, then another ECM coupling protocol should be followed. If the concentration is indeed low, say less than 500 µg/mL, then we may have to resort to placing the existing ECM in concentration tubes, followed by multiple high-speed centrifugations, to form a highly concentrated protein pellet that can then be resuspended to obtain a more desirable concentration.

4.3 What It All Means

When the field of embryogenesis first emerged in the nineteenth century, developmental processes were seen to arise from fundamentally physical processes acting on and around cells and tissues. But interestingly, these ideas were thrown into the ash heap of science over a half-century ago, and few have looked back since. Of those few is Donald Ingber, a pathbreaking developmental biologist at Harvard, who wrote, "These structural explanations fell by the wayside when biochemistry and molecular biology took hold and began to blossom. The power to switch on and off different embryological programs through genetic engineering clearly has confirmed the importance of specific genes for developmental control." He then went on to argue: "But identification of a light switch on a factory floor does not explain how a finely crafted automobile is constructed. Similarly, although we have solved the Human Genome, we still do not understand how embryonic tissues and organs are physically constructed with three-dimensional forms optimally designed to carry out their specialized functions" [52]. This antique view of development has, very recently, been shown to hold more true than molecular biologists or biochemists could have foreseen. My thesis can be seen as part of a collective effort to resuscitate the role of forces in both the development of tissues and cancer. But the fun is just beginning. I have brought TFM to Reed and attempted to show the spectacularly detailed information it can reveal to us about the dynamical, physical behavior of cells. I hope that future students—from both the Physics and Biology departments—can harness this powerful method to discover new insights about the mechanical behavior of cells.

References

[1] Bruce Alberts, Alexander Johnson, Julian Lewis, David Morgan, Martin Raff, Keith Roberts, and Peter Walter. *Molecular Biology of the Cell*. Garland Science, 2014.

[2] Sean B Carroll. *Endless Forms Most Beautiful: The new science of evo devo and the making of the animal kingdom*. Number 54. WW Norton & Company, 2005.

[3] E Bier. *The Coiled Spring*. Cold Spring Harbor New York: Cold Spring Harbor Laboratory Press, 2000.

[4] Mike Levine. Transcriptional enhancers in animal development and evolution. *Current Biology*, 20(17):R754–R763, 2010.

[5] Sorin Istrail and Eric H Davidson. Logic functions of the genomic cis-regulatory code. *Proceedings of the National Academy of Sciences of the United States of America*, 102(14):4954–4959, 2005.

[6] Michele A Wozniak and Christopher S Chen. Mechanotransduction in development: a growing role for contractility. *Nature Reviews Molecular Cell Biology*, 10(1):34–43, 2009.

[7] Rebecca L Siegel, Kimberly D Miller, and Ahmedin Jemal. Cancer statistics, 2015. *CA: A Cancer Journal for Clinicians*, 65(1):5–29, 2015.

[8] Douglas Hanahan and Robert A Weinberg. Hallmarks of cancer: the next generation. *Cell*, 144(5):646–674, 2011.

[9] Jan HJ Hoeijmakers. Genome maintenance mechanisms for preventing cancer. *Nature*, 411(6835):366–374, 2001.

[10] Bert Vogelstein, Nickolas Papadopoulos, Victor E Velculescu, Shibin Zhou, Luis A Diaz, and Kenneth W Kinzler. Cancer genome landscapes. *Science*, 339(6127):1546–1558, 2013.

[11] Robert Weinberg. *The Biology of Cancer*. Garland science, 2013.

[12] Isaiah J Fidler. The pathogenesis of cancer metastasis: the "seed and soil" hypothesis revisited. *Nature Reviews Cancer*, 3(6):453–458, 2003.

[13] Robert A Weinberg. *One Renegade Cell: The quest for the origins of cancer*. Basic Books, 2008.

[14] Brenton D Hoffman, Carsten Grashoff, and Martin A Schwartz. Dynamic molecular processes mediate cellular mechanotransduction. *Nature*, 475(7356):316–323, 2011.

[15] Diana E Jaalouk and Jan Lammerding. Mechanotransduction gone awry. *Nature Reviews Molecular Cell Biology*, 10(1):63–73, 2009.

[16] Dennis E Discher, Paul Janmey, and Yu-li Wang. Tissue cells feel and respond to the stiffness of their substrate. *Science*, 310(5751):1139–1143, 2005.

[17] Hongmei Yu, Janna Kay Mouw, and Valerie M Weaver. Forcing form and function: biomechanical regulation of tumor evolution. *Trends in Cell Biology*, 21(1):47–56, 2011.

[18] Sangyoon J Han, Kevin S Bielawski, Lucas H Ting, Marita L Rodriguez, and Nathan J Sniadecki. Decoupling substrate stiffness, spread area, and micropost density: a close spatial relationship between traction forces and focal adhesions. *Biophysical Journal*, 103(4):640–648, 2012.

[19] Patrick W Oakes, Shiladitya Banerjee, M Cristina Marchetti, and Margaret L Gardel. Geometry regulates traction stresses in adherent cells. *Biophysical Journal*, 107(4):825–833, 2014.

[20] Daniel J Müller and Yves F Dufrêne. Atomic force microscopy: a nanoscopic window on the cell surface. *Trends in Cell Biology*, 21(8):461–469, 2011.

[21] Ming Dao, Chwee Teck Lim, and Subra Suresh. Mechanics of the human red blood cell deformed by optical tweezers. *Journal of the Mechanics and Physics of Solids*, 51(11):2259–2280, 2003.

[22] Steven Munevar, Yu-li Wang, and Micah Dembo. Traction force microscopy of migrating normal and H-Ras transformed 3T3 fibroblasts. *Biophysical Journal*, 80(4):1744–1757, 2001.

[23] Benedikt Sabass, Margaret L Gardel, Clare M Waterman, and Ulrich S Schwarz. High resolution traction force microscopy based on experimental and computational advances. *Biophysical Journal*, 94(1):207–220, 2008.

[24] Casey M Kraning-Rush, Joseph P Califano, and Cynthia A Reinhart-King. Cellular traction stresses increase with increasing metastatic potential. *PloS One*, 7(2):e32572, 2012.

[25] Christopher R Jacobs, Hayden Huang, and Ronald Y Kwon. *Introduction to Cell Mechanics and Mechanobiology*. Garland Science, 2012.

[26] John Tyler Bonner. *The Ideas of Biology*. Courier Corporation, 2012.

[27] Louise P Cramer. Forming the cell rear first: breaking cell symmetry to trigger directed cell migration. *Nature Cell Biology*, 12(7):628–632, 2010.

[28] Bruce Alberts, Dennis Bray, Karen Hopkin, Alexander Johnson, Julian Lewis, Martin Raff, Keith Roberts, and Peter Walter. *Essential Cell Biology*. Garland Science, 2013.

[29] Edward D Korn, Marie-France Carlier, and Dominique Pantaloni. Actin polymerization and ATP hydrolysis. *Science*, 238(4827):638–644, 1987.

[30] Yu-Li Wang. Exchange of actin subunits at the leading edge of living fibroblasts: possible role of treadmilling. *The Journal of Cell Biology*, 101(2):597–602, 1985.

[31] Kenneth G Campellone and Matthew D Welch. A nucleator arms race: cellular control of actin assembly. *Nature Reviews Molecular Cell Biology*, 11(4):237–251, 2010.

[32] Miguel Vicente-Manzanares, Xuefei Ma, Robert S Adelstein, and Alan Rick Horwitz. Non-muscle myosin II takes centre stage in cell adhesion and migration. *Nature Reviews Molecular Cell Biology*, 10(11):778–790, 2009.

[33] Richard O Hynes. Integrins: versatility, modulation, and signaling in cell adhesion. *Cell*, 69(1):11–25, 1992.

[34] Richard O Hynes. Integrins: bidirectional, allosteric signaling machines. *Cell*, 110(6):673–687, 2002.

[35] Adèle De Arcangelis and Elisabeth Georges-Labouesse. Integrin and ECM functions: roles in vertebrate development. *Trends in Genetics*, 16(9):389–395, 2000.

[36] Benjamin Geiger, Joachim P Spatz, and Alexander D Bershadsky. Environmental sensing through focal adhesions. *Nature Reviews Molecular Cell Biology*, 10(1):21–33, 2009.

[37] Willis Li, Johanna Talavera Ohlmeyer, Mary Ellen Lane, and Daniel Kalderon. Function of protein kinase a in hedgehog signal transduction and drosophila imaginal disc development. *Cell*, 80(4):553–562, 1995.

[38] Silvia Aldaz, Luis M Escudero, and Matthew Freeman. Live imaging of drosophila imaginal disc development. *Proceedings of the National Academy of Sciences*, 107(32):14217–14222, 2010.

[39] Klaudia Giehl. Oncogenic Ras in tumour progression and metastasis. *Biological Chemistry*, 386(3):193–205, 2005.

[40] Martin Alexander Schwartz. Integrins and extracellular matrix in mechanotransduction. *Cold Spring Harbor Perspectives in Biology*, 2(12):a005066, 2010.

[41] Martin A Schwartz and Douglas W DeSimone. Cell adhesion receptors in mechanotransduction. *Current Opinion in Cell Biology*, 20(5):551–556, 2008.

[42] Huimin Zhang, Frédéric Landmann, Hala Zahreddine, David Rodriguez, Marc Koch, and Michel Labouesse. A tension-induced mechanotransduction pathway promotes epithelial morphogenesis. *Nature*, 471(7336):99–103, 2011.

[43] Ramsey A Foty and Malcolm S Steinberg. Measurement of tumor cell cohesion and suppression of invasion by E-or P-cadherin. *Cancer Research*, 57(22):5033–5036, 1997.

[44] Ramsey A Foty and Malcolm S Steinberg. Cadherin-mediated cell-cell adhesion and tissue segregation in relation to malignancy. *International Journal of Developmental Biology*, 48:397–410, 2004.

[45] Pengfei Lu, Valerie M Weaver, and Zena Werb. The extracellular matrix: a dynamic niche in cancer progression. *The Journal of Cell Biology*, 196(4):395–406, 2012.

[46] Hussein D Foda and Stanley Zucker. Matrix metalloproteinases in cancer invasion, metastasis and angiogenesis. *Drug Discovery Today*, 6(9):478–482, 2001.

[47] Mikala Egeblad and Zena Werb. New functions for the matrix metalloproteinases in cancer progression. *Nature Reviews Cancer*, 2(3):161–174, 2002.

[48] Peter Friedl and Darren Gilmour. Collective cell migration in morphogenesis, regeneration and cancer. *Nature Reviews Molecular Cell Biology*, 10(7):445–457, 2009.

[49] Peter Friedl and Stephanie Alexander. Cancer invasion and the microenvironment: plasticity and reciprocity. *Cell*, 147(5):992–1009, 2011.

[50] Robert W Style, Rostislav Boltyanskiy, Guy K German, Callen Hyland, Christopher W MacMinn, Aaron F Mertz, Larry A Wilen, Ye Xu, and Eric R Dufresne. Traction force microscopy in physics and biology. *Soft Matter*, 10(23):4047–4055, 2014.

[51] Yvonne Aratyn-Schaus, Patrick W Oakes, Jonathan Stricker, Stephen P Winter, and Margaret L Gardel. Preparation of complaint matrices for quantifying cellular contraction. *JoVE (Journal of Visualized Experiments)*, (46):e2173–e2173, 2010.

[52] Donald E Ingber. Mechanical control of tissue morphogenesis during embryological development. *International Journal of Developmental Biology*, 50(2/3):255, 2006.